

# A critical review of improved deep convolutional neural network for multi-timescale state prediction of lithium-ion batteries.

WANG, S., REN, P., TAKYI-ANINAKWA, P., JIN, S. and FERNANDEZ, C.

2022

© 2022 by the authors. Licensee MDPI, Basel, Switzerland.

Review

# A Critical Review of Improved Deep Convolutional Neural Network for Multi-Timescale State Prediction of Lithium-Ion Batteries

Shunli Wang <sup>1,2</sup> , Pu Ren <sup>2</sup>, Paul Takyi-Aninakwa <sup>2</sup> , Siyu Jin <sup>3</sup>  and Carlos Fernandez <sup>4,\*</sup> <sup>1</sup> College of Electrical Engineering, Sichuan University, Chengdu 610017, China; wangshunli@swust.edu.cn<sup>2</sup> School of Information Engineering, Southwest University of Science and Technology, Mianyang 621010, China; renpu@swust.edu.cn (P.R.); lingorocsta@hotmail.com (P.T.-A.)<sup>3</sup> Department of Energy Technology, Aalborg University, Pontoppidanstraede, 111 9220 Aalborg, Denmark; sji@et.aau.dk<sup>4</sup> School of Pharmacy and Life Sciences, Robert Gordon University, Aberdeen AB10-7GJ, UK

\* Correspondence: c.fernandez@rgu.ac.uk

**Abstract:** Lithium-ion batteries are widely used as effective energy storage and have become the main component of power supply systems. Accurate battery state prediction is key to ensuring reliability and has significant guidance for optimizing the performance of battery power systems and replacement. Due to the complex and dynamic operations of lithium-ion batteries, the state parameters change with either the working condition or the aging process. The accuracy of online state prediction is difficult to improve, which is an urgent issue that needs to be solved to ensure a reliable and safe power supply. Currently, with the emergence of artificial intelligence (AI), battery state prediction methods based on data-driven methods have high precision and robustness to improve state prediction accuracy. The demanding characteristics of test time are reduced, and this has become the research focus in the related fields. Therefore, the convolutional neural network (CNN) was improved in the data modeling process to establish a deep convolutional neural network ensemble transfer learning (DCNN-ETL) method, which plays a significant role in battery state prediction. This paper reviews and compares several mathematical DCNN models. The key features are identified on the basis of the modeling capability for the state prediction. Then, the prediction methods are classified on the basis of the identified features. In the process of deep learning (DL) calculation, specific criteria for evaluating different modeling accuracy levels are defined. The identified features of the state prediction model are taken advantage of to give relevant conclusions and suggestions. The DCNN-ETL method is selected to realize the reliable state prediction of lithium-ion batteries.

**Keywords:** lithium-ion battery; state prediction; artificial intelligence; deep convolutional neural network; feature identification; ensemble transfer learning



**Citation:** Wang, S.; Ren, P.; Takyi-Aninakwa, P.; Jin, S.; Fernandez, C. A Critical Review of Improved Deep Convolutional Neural Network for Multi-Timescale State Prediction of Lithium-Ion Batteries. *Energies* **2022**, *15*, 5053. <https://doi.org/10.3390/en15145053>

Academic Editors: Jong Hoon Kim and Anup Barai

Received: 29 May 2022

Accepted: 5 July 2022

Published: 11 July 2022

**Publisher's Note:** MDPI stays neutral with regard to jurisdictional claims in published maps and institutional affiliations.



**Copyright:** © 2022 by the authors. Licensee MDPI, Basel, Switzerland. This article is an open access article distributed under the terms and conditions of the Creative Commons Attribution (CC BY) license (<https://creativecommons.org/licenses/by/4.0/>).

## 1. Introduction

Lithium-ion batteries have the advantages of high energy density, high efficiency, long cycle life, and low self-discharge rate. They are widely used in electric energy storage and electric vehicles (EVs) compared to batteries with other chemistries. High-precision, fast, and real-time lithium-ion battery state prediction technology is the core technology to ensure safety, achieve reliability, and prolong the service useful life of lithium-ion batteries. It also has significant engineering value for the large-scale application of lithium-ion batteries. As the core function of a battery management system (BMS), state prediction plays a significant role in multiple scenarios. For instance, in terms of EVs, the accuracy of state prediction prevents over-charge and over-discharge, extends battery cycle life, and even affects the industrial development of EVs to a certain extent. In terms of consumer electronic products, accurate state prediction of a lithium-ion battery helps users flexibly

manage the battery's remaining available energy and ensure the convenience of using these products. For energy storage at power stations, the state of health (SOH) is one of the primary reference indices for the safe use of lithium-ion batteries. It also plays an essential role in maintaining the stable operation of the battery system and ensuring personal safety. Whenever the SOH of lithium-ion batteries in an energy storage system is not accurately predicted, it leads to overheating, combustion, and accidents. Lastly, it ensures that the operations of energy storage power stations and even power systems are safe and stable.

Research on the state prediction method of lithium-ion batteries has gradually become an essential topic in the field of battery management studies [1]. Accurately predicting the state of lithium-ion batteries ensures the economical, convenient, safe, and stable operation of equipment under several working conditions, which has become the focus of the majority of experts and scholars. Current battery state prediction methods are mainly applied to EVs, consumer electronics, and power system storage. However, they are rarely used in communication base stations or uninterrupted power supply for data centers, aviation, and military fields. Several kinds of prediction methods that are currently in use have their corresponding disadvantages, which need to be optimized. Therefore, it is urgent to improve the state prediction methods of lithium-ion batteries and verify them under different working conditions.

Experts and scholars have researched lithium-ion battery state prediction technology and put forward a series of methods that have achieved good prediction results. Currently, the methods for state prediction can be divided into the following four categories: experiment or direct measurement methods based on the traditional way of calculating the experiment test, such as the discharge test, open-circuit voltage (OCV), and ampere-hour (Ah) integral methods. Researchers use standard lab tests under the condition to establish the battery's mapping relationship between external characteristic battery parameters and the state of charge (SOC) through the use of a look-up table or simple calculation to predict the state of the lithium-ion battery. The model-based methods are based on the lithium-ion battery models established for the state observer, such as the Kalman filter (KF) and its advanced models, such as the extended Kalman filter (EKF), the unscented Kalman filter (UKF), the particle filter (PF), and the robust H-infinity ( $H_\infty$ ) filter. The characteristic parameters of these methods are determined by establishing the mathematical model for the lithium-ion battery with accurate Ah integral method calculation results to reduce the influence of system noise, measurement noise, and system uncertainties.

The data-driven method introduces AI methods such as machine and deep learning (DL) to construct the model vector feature state prediction of lithium-ion batteries. These models include multiple neural networks, support vector machine (SVM), long short-term memory (LSTM), and gated recurrent unit (GRU) models by utilizing the state change rule of a large amount of lithium-ion battery data. The digital-analog hybrid-driven methods for lithium-ion batteries established the hybrid prediction method of model and data complementary advantages by integrating mathematical models and large datasets, thereby realizing the improvement of lithium-ion battery state prediction accuracy [2]. Currently, battery state prediction based on data-driven methods has achieved remarkable results, which is the current research hotspot and the general trend for the future.

By evaluating several prediction methods in the existing literature, this paper considers the high-precision state prediction method based on deep convolutional neural network ensemble transfer learning (DCNN-ETL) as the most suitable strategy compared with traditional model-based and data-driven methods. Therefore, an improved state prediction model for lithium-ion batteries based on the DCNN-ETL is constructed in this paper. Different modeling methods are compared with key evaluation metrics such as the root-mean-square error (RMSE), mean absolute error (MAE), convergence speed, and accuracy. The main advantages of each model are highlighted by introducing specific evaluation criteria to achieve an accurate prediction of the battery's state. The DCNN-ETL for battery state prediction is analyzed in detail, and effective evaluation criteria are established to assess it using different methods. The life characteristic change process is analyzed to

serve as a reference for the technological advancement of battery state prediction. In addition to the DCNN-ETL, the prediction effects of other DL methods are compared and analyzed. The high-precision DCNN-ETL method is selected for additional implementation and validation.

## 2. Analysis of Various State Predictions of Lithium-Ion Batteries

### 2.1. Overview of the State-of-Charge Prediction

For the practical application of lithium-ion battery packs, safety, reliability, and durability are essential. Therefore, the BMS is essential to monitor the working condition and ensure the safe and suitable operation of lithium-ion batteries [3]. The BMS is a component integrating multiple functions for the effective and efficient management of lithium-ion batteries. In addition to monitoring basic parameters of the battery such as voltage, current, and temperature, the BMS uses various strategies to predict the state parameters, such as SOC and SOH. Among them, the battery's SOC prediction has always been a hot topic in the field of battery management research. Accurate SOC prediction is a direct representation of the current endurance, and it is also the cornerstone for predicting the SOH of lithium-ion batteries [4].

In the design of the BMS, there are also several research hotspots, such as solving the problem of inconsistent battery parameters, balancing the technology, and performing fault diagnoses on the lithium-ion batteries [5]. The SOC prediction is mostly discussed for lithium-ion batteries. However, it is difficult to design a perfect BMS for lithium-ion batteries because it requires a mature BMS to provide comprehensive functions and ensure reliability [6]. Due to its design, the BMS has some technical difficulties in the execution of the state prediction of lithium-ion batteries as a basic function. The accuracy of the state prediction method of the lithium-ion battery directly determines whether the BMS can work perfectly, which serves as a defense mechanism for the safety of users. Therefore, it is essential to study the state prediction method of lithium-ion batteries. The SOC of a battery pack indicates the remaining capacity or energy of the lithium-ion battery [7]. The SOC level is between 0 and 1, which is usually expressed as a percentage. When the battery is fully charged, the SOC is 1, whereas it is 0 when it is fully discharged. Its definition is mathematically expressed in Equation (1).

$$\text{SOC} = \frac{Q_r}{Q_n} \times 100\%, \quad (1)$$

where  $Q_r$  represents the current amount of capacity in the battery, and  $Q_n$  represents the rated capacity of the battery. Both parameters are measured in Ah, but the SOC is a unitless quantity. It is usually represented as 1 or 100% as a ratio of these parameters. The SOC reflects the usage range of the battery to a certain extent. It plays a significant role in improving battery efficiency, slowing down battery aging, and preventing over-charging and over-discharging. However, the SOC of the battery cannot be directly measured but must be calculated by prediction methods using measurable parameters such as current, voltage, and temperature. Currently, many studies have made efforts to find real-time, accurate, and reliable SOC prediction methods [8]. A large number of research results have emerged. Common methods include the Ah integral, the OCV, the data-driven, and the model-based methods [9]. It must be taken into account that the lithium-ion battery is affected by other factors during the charging and discharging process, such as the ambient temperature, the magnitude of the current rate, and the aging level [10]. Therefore, a more accurate calculation expression is proposed, as shown in Equation (2).

$$\text{SOC} = \frac{1 - \gamma Q_i}{Q_o}, \quad (2)$$

where  $Q_i$  is the amount of the battery's energy or capacity that has been discharged at the timepoint  $i$ , and  $\gamma$  is the battery efficiency parameter, which is obtained from the

experimental data. Accurately predicting the remaining battery power has always been the focus and difficulty of BMS. The need for the high-precision remaining energy prediction has always been a prerequisite for prolonging the service life of the lithium-ion battery and exerting the discharge efficiency. For instance, the temperature, SOC, and discharge at the previous moment affect the prediction of the remaining energy of the battery. Furthermore, polarization effects and battery life affect the state prediction, which results in a high level of nonlinearities for the battery model [11].

In EVs, the battery pack exhibits a high degree of nonlinearity. The SOC is affected by many factors such as discharge rate, battery temperature, self-discharge rate, and cycle times, resulting in difficulties in accurately predicting the SOC [12].

#### 1. Discharge rate

Under the condition that other influencing factors remain unchanged, the discharge capacity of the battery decreases with an increased discharge rate. This is because the active material inside the battery has a limited depth of action due to the thickness of the electrode. When a large current is discharged, a greater discharge rate results in a shallower depth of action and lower utilization rate, thus reducing the battery capacity, and vice versa [13].

#### 2. Battery temperature

Battery power and active material utilization rate increase with the rise in battery temperature, which is mainly caused by changes in electrolyte temperature performance. When the battery temperature rises, the viscosity of the electrolyte decreases, and the activity increases, which increases the ion diffusion movement ability. Lastly, an increase in the utilization rate of the active material means that the discharge of the battery's actual available power increases. Conversely, when the battery temperature decreases, the active material utilization rate decreases with the remaining power [14]. Therefore, the remaining power is directly proportional to the operating temperature of the battery. In real-time applications, the charging and discharging working temperature range of a lithium iron phosphate batteries is 0–45 °C.

#### 3. Number of cycles

After a period of use, the rated capacity of lithium-ion batteries decreases. First, the power increases, and it remains the same for a period, and then the power gradually decreases. For lithium iron phosphate batteries, the cycle life is generally expressed by the number of charge–discharge times when the total discharge capacity drops to 80% of the rated capacity [15].

#### 4. Self-discharge rate

Self-discharge, also known as charge retention capacity, causes the internal chemical reactions in the battery to reduce the battery's stored energy without any connection to an external circuit or load. Under the self-discharge of the battery, the SOC value decreases as the storage time increases [16]. Generally, the self-discharge rate is expressed as the percentage of capacity reduction per unit time. Its mathematical expression is shown in Equation (3).

$$I_{sdr} = \frac{C_a - C_b}{C_a \times T} \times 100\%, \quad (3)$$

where  $I_{sdr}$  is the self-discharge rate.  $C_a$  is the battery power before storage,  $C_b$  is the battery power after storage, and  $T$  is the battery storage period. The self-discharge rate of lithium-ion batteries is related to many factors, such as the number of cycles, ambient temperature, and storage time. It is generally derived and calculated by experimental methods.

The discharge process of power batteries in EVs has complex and dynamic electrochemical reaction processes. The battery's SOC value is affected by factors such as discharge rate, ambient temperature, internal resistance, and self-discharge rate. Meanwhile, these factors vary from each other. It changes as the number of cycles increases, which increases the difficulty of battery modeling and the SOC prediction method. Currently, the prediction

methods of battery SOC mainly include the discharge test, OCV, Ah integral, internal resistance measurement, and data-driven methods. These methods are introduced and analyzed in detail below [17].

#### 5. Discharge test method

The discharge test method is an experimental process that uses either constant or varying current rates to continuously discharge the battery until the terminal voltage reaches the discharge cutoff voltage. The battery capacity is equal to the product of the current discharge value and the discharge time. The discharge test method is often used in the laboratory. It is the most reliable SOC prediction method and is suitable for all types of batteries. However, it also has several defects that limit its application. First, it takes substantial measurement time. Only after the entire discharge test is over can the SOC value at each time be calculated, and real-time prediction of SOC cannot be achieved. Second, the previous work of the battery must be forced to stop and switched to constant current discharge rates. Therefore, the discharge test method is unsuitable for predicting the SOC prediction of power batteries with real-time prediction requirements. However, it is used for the maintenance of power batteries and the determination of battery model parameters [18].

#### 6. Open-circuit voltage method

The OCV method predicts the SOC value on the basis of the approximately linear relationship between SOC and OCV values of the battery. The actual operation process is as follows: first, the battery needs to stand for a long enough time to ensure the stability of its OCV and other parameters. Then, the OCV value of the battery is measured to obtain the SOC value according to the known approximate linear function relationship. The advantage of the OCV method is its simplicity and strong operability [19]. However, the OCV can only be obtained after the battery is fully rested, when the electrochemical reaction inside the battery is stable, which makes it impossible to track the SOC in real time. Although the functional relationship between SOC and OCV is relatively constant for a short time, the relationship between SOC and OCV changes with the aging of the battery, which also affects the accuracy of SOC prediction.

#### 7. Ampere-hour integral method

The Ah integral method predicts the SOC prediction of the battery by calculating the accumulated power of the battery during charging or discharging and compensating for the predicted SOC value on the basis of the temperature and the charge–discharge rate. It is currently the most commonly used and simplest SOC prediction method, and it has been successfully applied to the power prediction of electronic consumer products [20]. If the initial state of charging and discharging is specified as  $SOC_0$ , then the SOC value in the current state is calculated using Equation (4).

$$SOC = SOC_0 - \frac{1}{Q_n} \int_0^t \eta i dt, \quad (4)$$

where  $Q_n$  is the nominal capacity,  $i$  represents the battery current, which is positive when discharging and negative when charging, and  $\eta$  is the battery Coulombic efficiency, including the temperature influence coefficient  $\eta_r$  and the charge–discharge rate coefficient  $\eta_i$ . Three problems should be paid attention to when using the Ah integral method. The method itself cannot provide the initial battery value,  $SOC_0$ . Inaccurate current measurement increases the prediction error, which becomes larger and larger after long-term accumulation. The battery efficiency coefficient  $\eta$  must be considered when predicting the SOC. However, the accuracy of current measurement can be improved using high-performance current sensors, which greatly increases the cost of the system. Moreover, to solve the problem of battery's Coulombic efficiency  $\eta$ , it is necessary to establish empirical formulas for temperature influence coefficient  $\eta_r$  and charge–discharge rate coefficient  $\eta_i$  through a large number of experimental data. If the SOC prediction accuracy requirement

is not high, the Ah integral method can be applied to the measurement of the remaining battery power of EVs.

#### 8. Internal resistance measurement method

The internal resistance measurement method refers to the method of measuring the internal alternating current (AC) resistance of the battery by exciting the battery with different frequencies of AC and calculating the SOC value using the static battery model of the remaining power and the AC internal resistance. At the later stage of battery discharge, the internal resistance measurement method has high prediction accuracy and battery adaptability and is generally used in combination with the Ah integral method. However, this method only considers two aspects of discharge current and internal resistance. Thus, it does not consider the influence of environmental temperature, battery cycle times, the imbalance between battery cells, and other factors on the internal resistance of the battery. The cause of battery internal resistance is very complicated; accordingly, the internal resistance measurement method makes the final SOC accuracy not very high. Furthermore, there are differences in AC impedance at different current frequencies, and EV power batteries do not work at a fixed AC frequency. Consequently, the internal resistance measurement method cannot meet the SOC prediction requirements of lithium-ion batteries for EVs [21].

#### 9. Data-driven method

The neural network is an AI technology that has been developed in recent years and uses a simulation of brain signal processing. A neural network is a complex nonlinear system formed by a large number of simple neurons connected extensively. It can automatically summarize the collected data and obtain the internal characteristics of the data. It also has a nonlinear mapping capability and is suitable for noncausal relationships with more complex nonlinearities, such as identification, judgment, reasoning, and classification issues. The battery is a highly nonlinear system, and it is usually difficult to establish a reasonable and accurate mathematical model for its charging and discharging process [22]. Therefore, given external incentives, the data-driven method can use its self-learning ability and the parallel structure to simulate the nonlinear characteristics to predict the SOC value of the lithium-ion battery.

SOC prediction often uses a typical three-layer neural network structure, in which the number of neurons in the input and output layers is determined by the requirements of the actual system. Furthermore, the total number of neurons in the middle layer depends on the system complexity and the analysis accuracy requirements. The data-driven method uses inputs including battery voltage, ambient temperature, charging and discharging current, battery internal resistance, and accumulated discharge power. Whether the input type and quantity are reasonable or not, they directly affect the calculation cost and accuracy of the method model [23]. The disadvantage of the data-driven method is that experimental datasets are needed to train the parameters. However, the SOC prediction accuracy is significantly affected by the training data and the training method.

#### 10. Kalman filtering method

Lithium-ion batteries are a typical nonlinear system. With the development of the KF method, the improved KF can already be used in complex nonlinear systems. For the nonlinear KF method, there are mainly the EKF and UKF methods. Among them, the EKF method uses the partial differentiation method for linearization. It uses the partial differentiation method to generate the Jacobian matrix in each iteration cycle of the method; hence, the calculation is more complicated. Conversely, when the nonlinear state-space equation is linearized with the Jacobian matrix in the EKF method, if the system is highly nonlinear, the convergence results may deviate, which may lead to divergence of the prediction results [24]. The UKF method uses an unscented transformation to approximate the probability density distribution of state variables of the system. Compared with the EKF method, this transformation has certain advantages. Data transformation is not only

more accurate but also simple in calculation and easy to implement, which makes it more suitable for state prediction of nonlinear systems.

## 2.2. Overview of the State of Health Prediction

With the application of lithium-ion batteries in aviation, new EVs, civil power generation, and other fields, ensuring the safety and reliability of lithium-ion batteries under complex working conditions has become a critical issue in the field of lithium-ion battery research. Researchers use the SOH to indirectly represent the current performance of batteries. Hence, it is essential to accurately predict the SOH of lithium-ion batteries to extend the life of the battery while ensuring reliability throughout its life in real-time [25]. Battery SOH represents the ratio of the current battery capacity to the rated capacity of the new battery and refers to the state of the battery from the beginning to the end of life, which is expressed as a percentage. This is used to quantitatively describe the current performance of the battery [26].

There are many performance indicators for batteries. There are many definitions for SOH; therefore, the concept is not unified. Currently, the definition of SOH is mainly reflected in capacity, electric quantity, internal resistance, cycle times, and peak power. The automobile industry-standard “QC/T743-2006” issued by China in 2006 stipulates the conditions for the end of lithium-ion battery life, i.e., when the available capacity attenuates to 80% of the standard capacity [27]. Currently, SOH is generally recognized in the industry as shown in Equation (5).

$$\text{SOH} = \frac{Q_n}{Q_o} \times 100\%, \quad (5)$$

where  $Q_n$  represents the actual available capacity of the battery after it is put into use, and  $Q_o$  is the rated or nominal capacity of the new battery before it leaves the factory.  $Q_n$  decreases with the increase in the number of charge and discharge cycles.

In recent decades, extensive studies have been carried out on the capacity and SOH predictions of lithium-ion batteries, which can be divided into three types: empirical or electrochemical models, equivalent circuit models (ECMs), and data-driven models, which can be divided into micro and macro timescales according to the time perspective [28]. The micro timescale focuses on the state of single charge and discharge of lithium-ion batteries. The macro timescale focuses on data over the useful life period of the lithium-ion battery.

The empirical or electrochemical models mainly start from the electrochemical reaction mechanism of the battery itself and predict the SOH of the battery by studying the electrochemical law of the decline of the battery capacity [29]. This kind of method mainly builds the mechanism model of the battery according to the porous electrode theory and the concentrated solution theory. It describes the physical and chemical reaction process between the electrode and the active material surface. The model parameters related to degradation were identified using the measurement or system identification method to predict the SOH of the lithium-ion battery [30]. Commonly used electrochemical models include a two-dimensional quasi-electrochemical model, a single-particle model, and an extended single-particle model [31]. Compared with other models, the electrochemical model can better evaluate and simulate the key performance indicators of the power battery. However, there are many parameters related to the internal materials of the battery; thus, it is difficult to update and regularly calibrate in real-time applications. The model computation is high and generally only used for battery performance analysis. However, the simplified electrochemical model has reduced computational cost. The dynamic simulation accuracy is poor because the nonlinearities and the variation of the characteristic parameters of the battery with SOC are ignored.

An ECM is a battery model and method that replaces the actual and complex physical and chemical working process of the battery with an equivalent, simple, and easily researched physical or mathematical process under a condition. Therefore, the accuracy mainly depends on the adaptability of the model to the working process of the battery. The ECM is mainly from the perspective of electrical engineering to convert the lithium-ion

battery into an equivalent circuit model, and the corresponding relationship between the OCV and SOC is established. The dynamic characteristics and capacity decline characteristics of the battery are described using the measured operating voltage, current, and other external working conditions [32]. The core technology includes accurate measurement of battery internal resistance, which describes battery characteristics, and a prediction of the functional relationship between OCV and SOC [33]. The main research methods are KF and PF methods.

Although an ECM can effectively predict capacity under certain conditions by first simulating the battery's impedance, the battery internal resistance measurement results cannot be guaranteed under the condition of traceability, and the accuracy of such simulation results is not reliable. These technologies require several matrices and a high demand for computing resources, which hampers the real-time application. The data model can directly analyze the hidden SOH information and its evolution rule from the external characteristic parameters of lithium-ion batteries [34]. The battery data mostly come from the user process data and laboratory data, which contain the influence of various working states on the battery to reflect the individual differences to a certain extent and overcome the problem of poor adaptability of the ECM. Currently, such methods mainly include neural networks, SVM, and autoregressive models [35].

Currently, given the strong nonlinearity of lithium-ion batteries, the related research is mainly divided into two types of methods: model-based and data-driven methods to realize the health status [36]. The model-based method, which was established earlier, is a relatively mature mathematical method. It mainly establishes an ECM to simplify the complex internal reactions of the lithium-ion battery and then predicts the health status combined with intelligent state observers. The established models mainly include the electrochemical mechanism model, ECM, and empirical model. Internal factors such as the electrolyte concentration and SOC, as well as the influence of external factors such as temperature effects on the SOH, need to be considered [37]. Data-driven methods for the lithium-ion battery's SOH prediction are also making progress, using the backpropagation (BP) neural network and other neural networks to make discoveries. Compared with the mathematical model-driven method, the accuracy of the assessment of the SOH of lithium-ion batteries has significantly improved [38].

Even though much progress has been made in the field of lithium-ion battery condition assessment at this stage, due to the dynamic nature of the lithium-ion battery itself and various complex working conditions, it is difficult to achieve a high-precision simulation of the real working conditions and the SOH [39]. There is also a lack of uniform measurement standards, and the relevant studies and applications are still in an immature state [40].

### *2.3. Overview of the State-of-Power Prediction*

The state-of-power (SOP) prediction of the battery is an essential part of the BMS of the power battery pack. The accuracy of the SOP prediction directly affects the user's judgment of the vehicle information, which affects the normal operation of the vehicle [41]. For an in-depth study, SOP is used to describe the peak charge–discharge power of the battery in its current state. The peak power of the battery can be predicted by evaluating the charge–discharge limit capability of the battery. The SOP guides the lithium-ion battery pack to optimally match the power performance of external equipment and provide an effective safety guarantee and power output for the equipment and battery pack within a safe range. It also helps maximize the braking energy recovery function of the motor [42]. The prediction of SOP helps to prevent over-charge and over-discharge in advance and has significant theoretical and practical value for prolonging the service life of the batteries.

The test conditions for battery peak power mainly include the United States Advanced Battery Consortium (USABC) test manual, the HPPC test proposed by the Freedom CAR project, the JEVS power density test, and the power test proposed by the Chinese Ministry of Science and Technology in the battery test specification. The core of the USABC test is the peak power test of the battery. The battery is discharged to a different depth of discharge

(DOD), and then the battery is continuously discharged for  $t$  seconds to reach the battery discharge cutoff voltage,  $U_{min}$  [43]. For the HPPC test, when the battery is continuously discharged at a constant current for  $t$  seconds, the terminal voltage drops to the battery discharge cutoff voltage,  $U_{min}$ . Then, the constant current value is the peak current of the battery in that state.

The objects tested by the JEVS power density test are mainly lithium-ion and nickel-metal hydride batteries. For this test, the peak power at different power levels is from 0% to 100% [44]. The batteries are charged alternately at different rates. After discharging, the voltage–current fitting curve is used to find the highest charging voltage and the lowest discharging voltage of the battery at different depths of discharge. Then, the peak power of the battery is obtained by substituting the corresponding calculation formula [45].

The peak power of the battery refers to the product of the voltage value and the current value collected by the BMS every 0.1 s [46]. The average power of the battery at 1, 3, 5, and 10 s is calculated by dividing the accumulated peak power by the discharge time [47]. According to the different uses of the battery, different continuous discharge times are defined. For hybrid EVs, high-current continuous discharge is required for 10 s. For battery EVs, continuous discharge is required for 30 and 60 s [48].

Currently, the research on the battery power state mainly focuses on the impact of a single factor on the peak power of the battery and the maximum power during the entire battery usable period [49]. Researchers have analyzed the influence of battery power, temperature, and terminal voltage on battery power. It can be concluded that temperature has the most influence on the prediction of SOP [50]. Some studies proposed multi-dimensional dynamic control methods to predict the battery voltage to calculate the available battery power. Some studies suggested that the predicted variables, such as SOC and aging, are not accurate values. However, these parameters are directly used in the battery model to predict the online peak power of the batteries [51]. Later studies put forward an electrochemical model that considers the influence of temperature on internal resistance and capacity [52]. The EKF method was used to predict the SOP of the lithium-ion battery, and the maximum peak power of the charge state and the minimum discharge states were obtained through multiparameter constraints [53].

#### 2.4. Overview of the State-of-Energy Prediction

Accurate state-of-energy (SOE) prediction seems to be more complicated and challenging compared to SOC prediction due to the consideration of nonlinear battery equilibrium potential [54]. In recent times, extensive attempts have been made to improve the effectiveness of SOE prediction. The main SOE prediction methods, with their advantages and disadvantages, are shown in Figure 1.

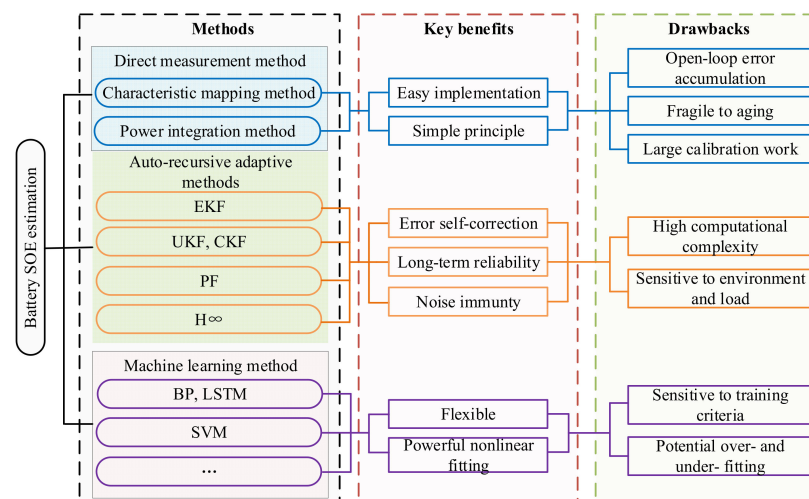


Figure 1. SOE prediction methods in terms of key benefits and drawbacks.

In Figure 1, it can be observed that the SOE prediction methods commonly used can be roughly divided into three categories: the power integration method, the data-driven prediction method, and the model-based method [55].

#### 1. Power integration method

The power integration method is simple to calculate and implement and is often taken advantage of to predict the SOE of a battery. However, this method has obvious drawbacks. Firstly, it is difficult to obtain the initial value of the battery SOE accurately [56]. In the power integration method, an inaccurate initial value is utilized to predict the SOE, which easily causes the accumulation of errors [45]. Secondly, the method is sensitive to the accuracy of the current sensor. The working conditions of lithium-ion batteries are complex, and the sensor is often affected by uncontrollable factors such as external temperature and noise, resulting in accumulated errors in the integration process. Lastly, the method has a high dependence on the initial energy value of the battery [57]. Nevertheless, the aging of the battery leads to energy attenuation, which reduces the reference energy, resulting in a decrease in the prediction accuracy of SOE [58]. The mathematical expression of the power integration method is shown in Equation (6).

$$\begin{cases} \text{SOE}(t) = \text{SOE}(t_0) + \frac{1}{En} \int_{t_0}^t u I dt \\ \text{SOE}(t) = \text{SOE}(t_0) + \frac{u I \Delta t}{En} \end{cases} \quad (6)$$

Equation (6) shows the continuous and discrete forms of the power integration method, where  $\text{SOE}(t)$  refers to the energy state value at the current moment, and  $\text{SOE}(t_0)$  is the initial energy state value.  $En$  is the rated energy of the battery, and  $I$  represents the charging and discharging current of the battery under actual operating conditions. Due to the shortcomings of the power integration method, scholars have proposed a series of improvements, such as solving the SOE value by constructing the mapping relationship among the discharge power, OCV, residual energy, and the SOE [51].

#### 2. Data-driven SOE prediction method

With the rise of machine learning techniques, data-driven methods are widely used in battery SOE prediction. For example, a BPNN was used to capture the nonlinear and coupled properties of the battery, considering irreversible energy losses due to Joule heating, electrochemical reactions, and phase shifts [59]. Similarly, considering the effects of temperature and discharge rate, a wavelet neural network model was applied to simulate battery electrodynamics. Furthermore, methods such as LSTM and SVM are used for SOE prediction. The prediction effect of these types of methods depends to a large extent on the quantity and quality of training data and the choice of fitting method, which requires a large amount of computation and high sensor accuracy [49].

#### 3. Model-based SOE prediction method

Scholars have proposed many SOE prediction methods based on the state-space model to overcome the shortcomings of the power integration method. This method first establishes the ECM of the battery, such as the Thevenin model, the second-order resistor-capacitor (RC) model, or the composite ECM [60]. Then, it selects the appropriate observer or filter for SOE prediction, such as the EKF, UKF, CKF, PF,  $H\infty$ , and other corresponding optimized methods [61].

#### 4. Extended Kalman filter

The EKF method is an improvement of the traditional KF method by expanding the linear system. The first-order Taylor series expansion is used, while ignoring the higher-order terms. The method can be applied to nonlinear systems such as lithium-ion batteries. The method iterates the state vector at the current moment according to the predicted value of the state vector at the previous moment and the output observation value at the next moment. Moreover, the error covariance is updated, and the state vector is gradually

corrected by the coefficient gain such that the result is close to the true value. The structure of the EKF method is simple and easy to understand, and it is one of the most widely used SOE prediction methods. The second-order RC model is shown in Figure 2 as an example, taking SOE,  $U_1$ , and  $U_2$  as state variables, and the terminal voltage  $U_L$  as the observation variable.

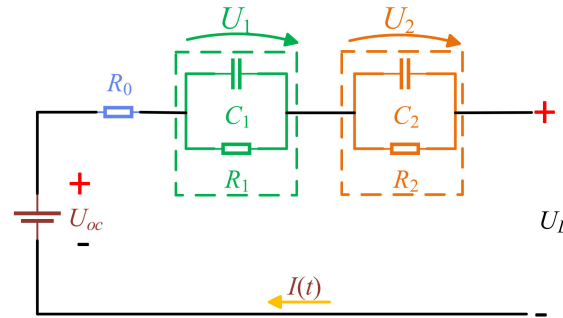


Figure 2. The second-order resistor–capacitor equivalent circuit model.

Figure 2 shows the second-order RC ECM, where  $U_{OC}$  represents the OCV of the battery, and  $U_L$  indicates the terminal voltage of the battery.  $R_0$  is the internal ohmic resistance of the battery, which is used to characterize the instantaneous voltage drop caused by the battery current.  $R_1$  and  $R_2$  are polarization resistances, and  $C_1$  and  $C_2$  are the polarization capacitances of the battery.

$$\begin{cases} \begin{bmatrix} \text{SOE}_k \\ U_{1,k} \\ U_{2,k} \end{bmatrix} = \begin{bmatrix} 1 & 0 & 0 \\ 0 & e^{\Delta t/\tau_1} & 0 \\ 0 & 0 & e^{\Delta t/\tau_2} \end{bmatrix} \begin{bmatrix} \text{SOE}_{k-1} \\ U_{1,k-1} \\ U_{2,k-1} \end{bmatrix} + \begin{bmatrix} -\frac{\eta U_{L,k-1} \Delta t}{E_N} \\ R_1 (1 - e^{\Delta t/\tau_1}) \\ R_2 (1 - e^{\Delta t/\tau_2}) \end{bmatrix} I_{k-1} + w_k \\ U_{L,k+1} = g(\text{SOE}_k) - U_{1,k} - U_{2,k} - I(k)R_0 + v_k \end{cases} \quad (7)$$

where  $\eta$  is the Coulombic efficiency, which is generally defined as 1 during the discharge process,  $\tau$  represents the time constant,  $w_k$  is the system noise, and  $v_k$  is the expression of the measurement noise.  $U_L$  represents the terminal voltage of the battery ECM.  $g(\text{SOE}_k)$  is the functional relationship between the OCV and SOE. The prediction process based on the EKF method can be divided into two parts: the prediction stage and the correction stage. The expression of the prediction stage is shown in Equation (8).

$$\begin{cases} \hat{X}_k^- = A \hat{X}_{k-1} + B I_{L,k-1} + w_k \\ \hat{P}_k^- = A \hat{P}_{k-1} A^T + Q_w \end{cases} \quad (8)$$

In Equation (8),  $A$  is the state transition matrix,  $B$  is the control-input matrix, and  $P$  indicates the prior error covariance matrix. The expression of the correction stage is shown in Equation (9).

$$\begin{cases} K_k = \hat{P}_k^- C_k^T (C_k \hat{P}_k^- C_k^T + R_k)^{-1} \\ \hat{X}_k = \hat{X}_k^- + K_k [Z_k - h(\hat{X}_k^-)] \\ \hat{P}_k = (1 - K_k C_k) \hat{P}_k^- \end{cases} \quad (9)$$

In Equation (9),  $Z_k - h(\hat{X}_k^-)$  represents the innovation at the current moment, i.e., the difference between the actual terminal voltage and the analog terminal voltage in the prediction process,  $I$  is an identity matrix, and  $C$  represents the system output matrix. The correction stage includes the Kalman gain update, state estimate update, and error covariance matrix update.

The SOE prediction process based on the EKF method is an auto-recursive “prediction–correction” method. Firstly, the predicted value is calculated, and then the predicted value is updated on the basis of the innovation and Kalman gain obtained from the observed value. The prediction can be obtained from the filtering value, which is obtained from the

prediction. The filtering and prediction interact, do not require any observation data to be stored, and can be processed in real-time applications.

The EKF method is less complex but has significant disadvantages. When the EKF method is used in a nonlinear system such as a lithium-ion battery, it linearizes the system. The specific implementation method is to perform a Taylor series expansion of the nonlinear equation but discard the high-order terms to use the linear Kalman method. However, when the high-order terms of the Taylor series expansion of the nonlinear equation contain a large amount of system information, blindly discarding the high-order terms can introduce a large linearization error. This reduces the accuracy of the method to predict the SOC and even causes filter divergence.

#### 5. Cubature Kalman filtering method

The cubature Kalman filtering (CKF) method is based on the third-order spherical radial volume criterion. It uses a set of volume points to approximate the state mean and covariance of nonlinear systems with additional Gaussian noise. The method is the closest approximation method to Bayesian filtering and can effectively solve the problem of nonlinear system state prediction. The method does not need to ignore high-order terms through Taylor series expansion and linearizes the nonlinear system. The prediction accuracy is higher than that of the EKF method [59].

The UKF and CKF methods do not need to linearize the nonlinear equation. The linearization error is eliminated, and the accuracy is greatly optimized compared to the EKF method. The UKF method transforms the linearization method of omitting high-order terms from the Taylor series expansion of nonlinear equations into an approximation of the eigenvalues of probability and statistics of nonlinear equations. There is no strict mathematical theory as the basis. Moreover, for the same sampling filtering method, UKF and CKF methods need to generate a point set through a certain sampling method in each iteration process. The point set size of the UKF method is  $2n + 1$ , while the volume point set of the CKF method is only  $2n$ . That is, each iteration is one sampling point less than the UKF method. Hence, theoretically, the CKF method has higher execution efficiency and better real-time performance.

In summary, the CKF method is superior to both the EKF and UKF methods in practicality, theoretical basis, time complexity, and reliability, which makes it very suitable for the SOE prediction of lithium-ion batteries [49].

#### 6. Particle filter

The PF method obtains the posterior probability density distribution of the state vector of the system. Then, it approximates the probability density function (PDF) by finding a set of random sample values propagated in the state space to replace the integral operation with the mean value of the sample. After the state update and time update, the weight and position of the particles are continuously adjusted on the basis of system observation. The initial conditional distribution is updated through the adjusted particle information. When the number of particles is large enough, the probability density distribution function of the updated particles gradually approximates the PDF of the state. The mean value of the particles approximates the predicted value of the state vector.

In terms of SOC and SOE prediction, compared with other Bayesian filters. The main advantage of the PF-based method is that it can be applied even if there is uncertainty in non-Gaussian measurements. The approximate PDF is obtained through the obtained approximate PDF. The requirements for the system model of the PF are lower compared to those of the KF methods in real-time applications. The PF does not require the model used to be linear and has a wide range of applications in solving nonlinear problems. However, the method requires a large amount of calculation and is prone to particle degradation. Hence, it needs to be further optimized when predicting the state of lithium-ion batteries [61].

## 7. Multistate collaborative prediction

Lithium-ion battery states are coupled and interact with each other. The multistate joint prediction and prediction can obtain more accurate results considering the multiple coupling of the electrothermal and aging conditions inside the battery. Furthermore, the BMS monitors various states of the battery, including the SOC, SOE, and SOH. Hence, the multistate collaborative prediction is aligned with the actual needs [62].

Domestic and foreign researchers have conducted extensive research on multistate joint prediction. The collaborative co-prediction of SOC and SOH is dominant in the existing literature. The main reason is that, with the continuous use of the battery, the capacity and internal resistance change. The rated capacity and internal resistance of the battery influence the SOC. The regular update of the SOH (capacity or resistance) can improve the accuracy of SOC prediction [63].

In addition to the joint prediction of SOC and SOH, some researchers also dealt with other two-state predictions, such as co-prediction of SOC and SOP, co-prediction of SOC and state of temperature (SOT), and co-prediction of SOE and SOP. Compared to predictions with only one state application, multistate prediction scenarios require more computational effort. Hence, designing simpler and more accurate ECMs and more advanced state prediction methods such as multi-timescale predictors will be the significant direction of future research [64].

## 3. Deep Convolutional Neural Network for State Prediction

In this section, the main state prediction features are analyzed for the DCNN method, introducing the specific indicators for evaluating the modeling accuracy and computation cost to evaluate the state prediction effect.

### 3.1. Mathematical Modeling of Deep Learning

A wide range of DL methods are used to predict the state of lithium-ion batteries. Compared with a feedforward neural network (FNN), an extreme learning machine (ELM) has a single hidden layer, fast learning speed, and effective generalization performance, and it introduces the idea of generalized learning (GL) [65]. An enhanced ELM model was constructed by nonparametric aging analysis to realize the storage and cyclic operation of the experimental data. The improved Gaussian regression and nonlinear regression were used to construct a multi-timescale framework to predict battery SOH [66]. A collaborative Gaussian processing regression model for capacity trend transfer learning between batteries was established. An improved DL method was proposed to describe online capacity variation.

An intelligent wavelet-antagonistic depth hybrid model was established to accurately predict solar power generation. Reinforcement learning and odorless transformation have also been introduced into random multicarrier energy management in smart devices [67]. A renewable microgrid energy management model based on an advanced machine learning model was established by considering the charging requirements of hybrid EVs. A DCNN was established to predict the battery power. A high-precision detection method based on the enhanced recurrent neural network was proposed for transmission line defect identification [68].

A state prediction was carried out using a DL data-driven method for preliminary data-driven processing to predict the battery state. Machine learning (ML) methods, including SVM, k-nearest neighbor (k-NN), artificial neural network (ANN), and linear regression (LR) methods, were applied to extract the degradation pattern recognition of lithium-ion batteries using impedance spectrum [69]. Combining the effective variables and LSTM with variable input sizes with other feature samples to achieve adaptive time series prediction and online verification, a DL method was implemented. An iterative deep neural network (DNN) framework was constructed for battery state prediction, in which two LSTM layers were established for feature extraction, LSTM1 and LSTM2 [70]. Battery parameters had the same size in each layer, making it highly scalable for different network input sizes. The overall framework of the DL prediction model is shown in Figure 3.

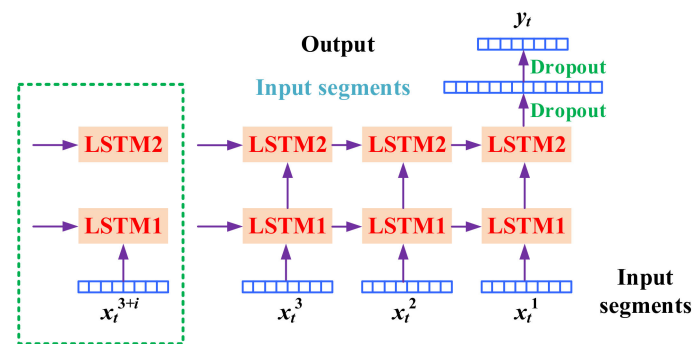


**Figure 3.** The whole framework of the DL prediction process.

As shown in Figure 3, a different number of data features are prepared for each sampling process according to the prediction model structure. When these samples are fed into the network, the data segment is used as the input for each LSTM unit. Hence, the network structure adapts to different input sampling sizes. When using  $n = 3$  as the processing input window size number, the LSTM1 cells with the same parameters are connected to the first layer, and the second layer, LSTM2, follows a similar pattern. The structure of the LSTM cells changes when different data segments are processed because multiple samples are obtained from a single tag to expand the available training dataset [71]. On the basis of the real-time validation results of the measured data, the prediction model structure is adjusted to achieve better performance. After feature extraction of the two LSTM layers, the output of the last LSTM2 cell, which contains information extracted from the entire input matrix, is used for further state prediction [72]. Then, a full connection layer containing neurons is used on top of the future prediction network. This expression is described as a mathematical function, as shown in Equation (10).

$$\hat{Y}_t^n = \{\hat{S}_{t+k}\}, k = 1, 2, \dots, n_p, \quad (10)$$

where  $\hat{Y}_t^n$  is the predicted matrix at timepoint  $t$  with sample count  $n$ , by state parameter  $\hat{S}_{t+k}$  of  $t$ , offset from 1 to  $n_p$  composition. In this paper, the state prediction method and mathematical and experimental analysis of an advanced BMS are presented. The deep Gaussian regression is taken advantage of to predict the health status degradation prediction of lithium-ion batteries. Combined with the integration and transfer learning of lithium-ion batteries, an improved DCNN model is established. The 10 year daily cycle data of eight implantable lithium-ion batteries are used as the dataset for the first time, and sub-models of the DCNN are pretrained using the dataset. The overall framework of the DCNN prediction process is presented in Figure 4.

Figure 4 shows the DCNN-ETL sub-models and implements state prediction using a comprehensive computational strategy, which is a pretrained DCNN model that plays a significant role in the iteration. Accurate state prediction of the state largely depends on ECM. The ECM uses the voltage responses to simulate the internal reactions and electrochemical processes of the lithium-ion battery. The influence of temperature change on the model structure is analyzed by combining the electrochemical model and the ECM with a high-precision feature description. On this basis, the distributed feature modeling is utilized to describe the battery's life cycle characteristics, and its performance serves as the foundation for the state-space equation. Using the mathematical description of the test results, the ECM of battery life cycle operating conditions is constructed, which provides a theoretical basis for the state-space equation at a wide temperature range. Through several experiments, the key factors are analyzed. Then, the model effectively simulates the characteristics of the battery.

Battery characterization and state prediction are effectively realized by the iterative application of terminal voltage and current. On the basis of the experimental tests of various working conditions, the various rules of each parameter are obtained. Then, an

improved state prediction framework is established by combining mathematical state-space description with model parameter identification. The time-varying parameters of the battery are affected by several environmental factors; hence, the model includes an RC circuit. Because the time-varying battery state contains stimulus factors, online parameter identification based on measured voltage and current data produces a stress response to external factors that effectively reflects the battery's dynamic characteristics [73].

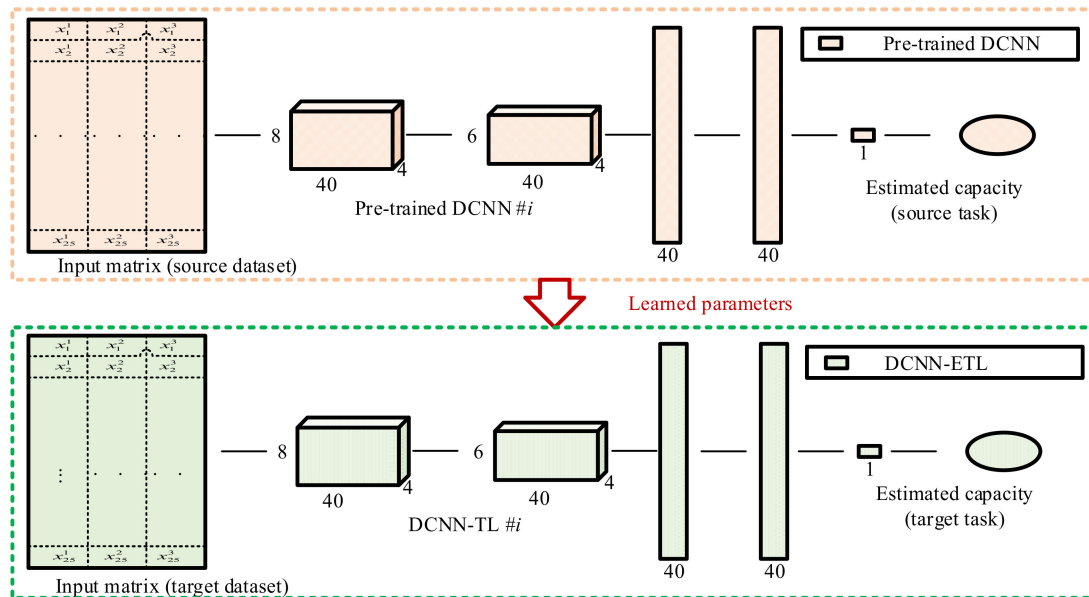


**Figure 4.** The overall framework of the DCNN-ETL prediction process.

### 3.2. DCNN-Based Calculation Framework

A neural network is an operational model consisting of a large number of nodes and the connections between them. Each node represents a specific output function, called the activation function. Each connection between two nodes represents a weighted value of the signal passing through the connection, called weight, which is equivalent to the memory of an ANN. The output of the network depends on the connection mode of the network. The weight and excitation functions are different. The network is usually an approximation of some method or function in nature and may also be an expression of a logical strategy [74].

The factors affecting the battery's SOH include the temperature, discharge depth, and charging rate. However, these indicators cannot directly represent the performance degradation degree of lithium-ion batteries, making it difficult to detect the SOH online [75]. The actual battery capacity refers to the electric energy stored when the battery is fully charged, which is an essential parameter that can directly represent the degradation of the battery. Therefore, it is often used as a health indicator to describe the degradation degree of a battery's SOH [76].

The battery capacity data are easy to collect and directly reflect the SOH of the battery. Therefore, the battery capacity is used as the SOH indicator to describe the degradation trend [77]. Figure 5 shows the overall flowchart of the DCNN-based SOH prediction method.

The DCNN process includes the obtained data sample features and the updated weight position coefficients of particles. The previous empirical distribution is modified on the basis of the measurement results of the weight position coefficient [78]. With the same SOH prediction accuracy, the number of particle samples is reduced, thus reducing the amount of calculation. The learning is transferred into knowledge learning from the input dataset and encoded as parameters of the  $n$ -single DCNN sub-model, as shown in Equation (11).

$$\theta^S = \{\theta_1^S, \theta_2^S, \dots, \theta_n^S\}. \quad (11)$$

In Equation (11), the overall calculation of the DCNN modeling particle-matrix  $\theta^S$  is composed of  $n$  single DCNN sub-modeling factors of  $\theta_n^S$ , where  $n$  is the number of single DCNN sub-models. Then, the pretrained DCNN model is transferred into the DCNN-TL model, and each step includes five convolution layers and three fully connected layers. Furthermore, this type of learning for the prediction of the state is used to achieve effective capacity prediction performance of internally connected lithium-ion cells. The TL method is to adjust the pretrained DCNN model through the dataset in the source task. Since long-term cyclic experimental testing is feasible, short-term cyclic experimental testing is carried out to make the model perform well in the target task. This enables efficient knowledge transformation with a smaller dataset, thus reducing the need for data collection and maintaining stable prediction accuracy. After the TL step is completed,  $n$  CNN-TL sub-models are established on the basis of the learning parameters of the DCNN model. Then, the whole framework of the CNN-ETL model is obtained by ensemble learning, including  $n$  CNN-TL sub-models, one fully connected layer, and one regression layer. The framework of the TL is shown in Figure 6.

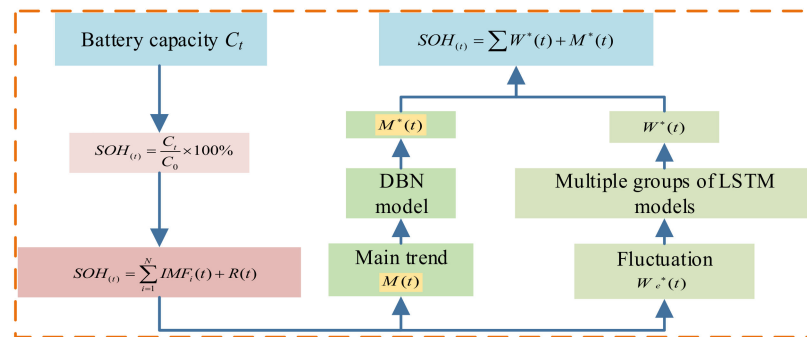


**Figure 5.** The overall flowchart of the DCNN-based SOH prediction method (“\*” is a special symbol that is used to characterize new values different from  $M$  and  $W$ , which have been calculated by DBN and LSTM algorithms).

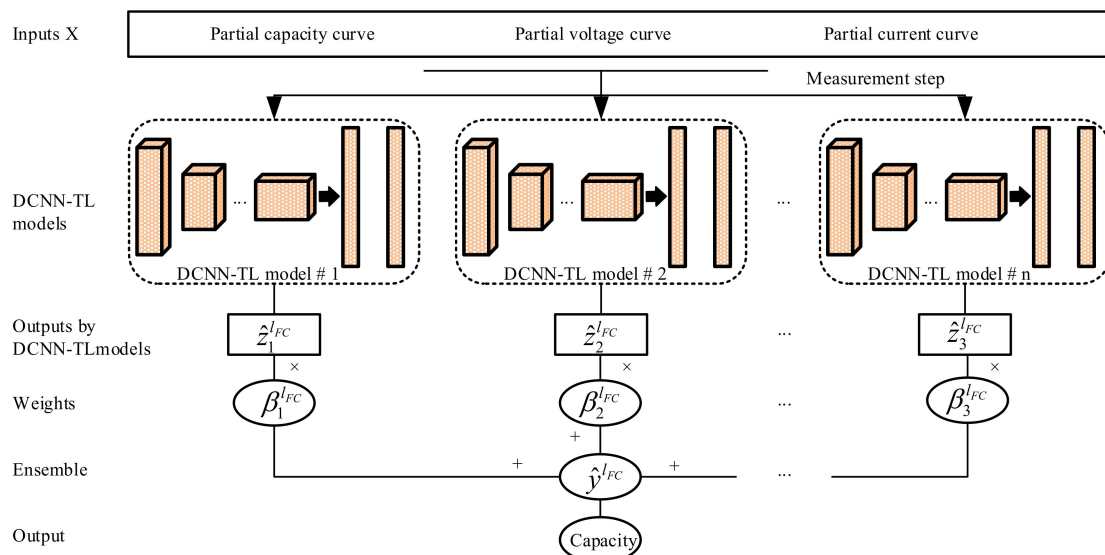


**Figure 6.** The flowchart of the iterative DCNN-based residual capacity prediction.

In Figure 6, the flowchart of a single DCNN-TL model is constructed from the DCNN-ETL modeling process. First, the input matrix  $X$  should be entered into each sub-model. Second, the convolution layer uses the  $k$  of the convolution operation  $C(X, K)$  to check the input matrix  $X$  for correction. The filter moves horizontally and vertically as  $X$  changes, and similar computational processing should be performed for each data point of the

sampled features. The  $i$ -th and  $j$ -th columns of the convolution layer's  $k$ -th output are shown in Equation (12).

$$\begin{cases} Z_{i,j,k}^{l,conv} = C(X, K)_{i,j,k} = \sum_{r=1}^{k_h} \sum_{s=1}^{k_w} \sum_{t=1}^{k_c} x_{i',j',t'} k_{r,s,t',k} + b_k \\ i' = (i - 1)S_h + r \\ j' = (j - 1)S_w + s \end{cases}, \quad (12)$$

where  $k_{r,s,t',k}$  and  $s$  represent the weight and deviation of  $k$  kernel at the convolution layer, respectively. The state-space model is used to predict the SOH of the lithium-ion battery. A new dataset is generated when constructing a state-space equation for each particle. Then, the matched particles are extracted to generate a new dataset. When the system gets the updated observations, the state-space equation generates a new set of particles. Therefore, the predicted value is obtained on the basis of the observation equation. The error between the actual and the predicted values for each particle feature is calculated using the observation equation. The one-step iterative framework of the sub-model of the DCNN-TL is presented step by step in Figure 7.

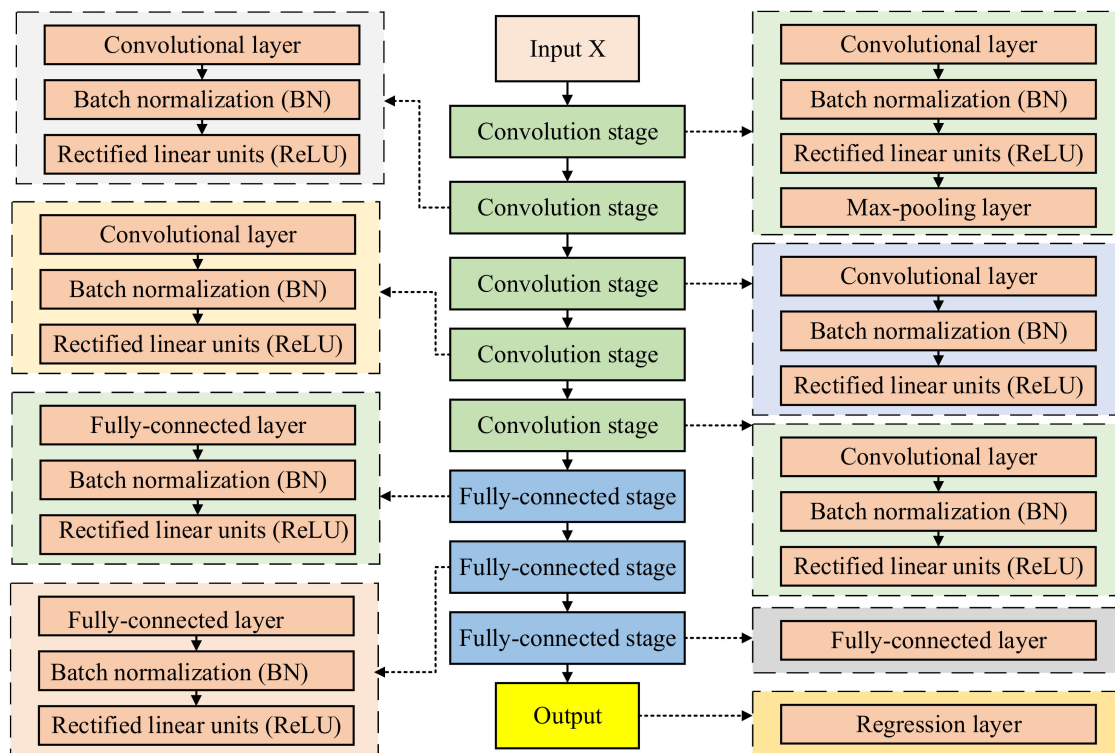


Figure 7. The one-step iterative framework of the DCNN-TL sub-models.

In Figure 7, the significance of the DCNN method is that there is no strict data length requirement in the calculation process. Thus, it can predict time-varying dynamic parameters with high precision and accurately extract discrete random samples. These particles use the possible density functions to complete the average prediction and data sampling feature processes to achieve effective time-varying model parameter prediction. Therefore, it is suitable for complex environmental effects. The steps of the resampling method are realized. The weight of each particle is calculated using Equation (13).

$$q(\chi_k | x_{0:k}(i), y_{1:k}) = p(x_k | \chi_{k-1}(i)). \quad (13)$$

In Equation (13), combined with theoretical analysis, simulation, and experimental verification, an improved model adapted to complex and wide temperature range conditions

is established. This model requires only a few effective particles and performs iterative calculations with a set threshold. If the number of effective particles is less than the set threshold, the model needs to be re-established. After sampling, the corrected particles are reselected so that a new set of particles can be formed using these selected particle features. Then, a posterior prediction is made for the system before resampling. The calculation process is realized on the basis of the posterior prediction effect, as shown in Equation (14).

$$w_t^{(i)} = (w_{t-1}^{(i)})^\alpha \frac{p(z_t | x_t^{(i)})p(x_t^{(i)} | x_{t-1}^{(i)})}{q(x_t^{(i)} | x_{t-1}^{(i)}, z_{1:t})}, \tag{14}$$

where  $\alpha$  is the annealing parameter of the genetic method, which is used to control the influence of the weight factor to reduce sample computation. The modeling effect is evaluated by considering the representation accuracy and computational complexities according to the requirements of state prediction. Therefore, using the experimental data measured in real time, the modeling process has strong applicability. Moreover, an equilibrium parameter is introduced to characterize the capacity difference between inner connected cells. Combined with the advantages of various construction methods, the modeling is improved. The function relation and mathematical state-space equation are calculated iteratively. During the experimental tests, the discharge capacity and time can be adjusted by changing the number of resistors added to the main circuit.

### 3.3. Application Analysis from Other Studies

The migration neural network (MNN) was designed to predict the aging trajectory of a battery that is adaptive to the pulse current working conditions. The SOH value of lithium-ion batteries is predicted using the ANN. Empirical mode decomposition is also used in the prediction process [79]. The improved ELM method is used to predict SOH, but the DNN method can also be used. The extensive ELM method is also used to predict the capacity of lithium-ion batteries [80]. An SOH prediction method was proposed using the fusion model and attention mechanism, which uses linear regression, SVM, adaptive nonattention mechanism LSTM, attention mechanism LSTM, and experimental verification [81].

From the microgrid application, grid battery life management can be used to improve the performance of EVs. The hybrid state prediction is conducted to realize the state optimization of different lithium-ion battery formulations. The case-based transfer learning is conducted to design the state prediction model for different battery formulations [82]. Average Euclidean distance (AED) and stacked denoising autoencoder (SDA) methods are used as powerful DL prediction methods. Using a nonuniform sampling of power data and DNN, a noninvasive load monitoring method was proposed [83]. The schematic and framework of the LSTM-based state prediction network can be described as shown in Figure 8.

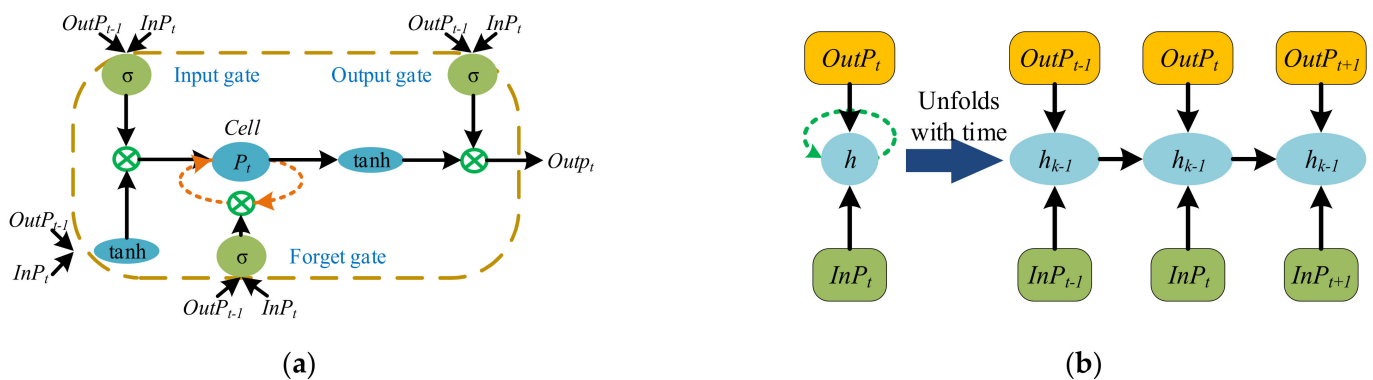


**Figure 8.** The schematic and framework of the LSTM-based state prediction network. (a) LSTM prediction schematic network. (b) The unfolded LSTM-RNN architecture.

The CNN is used to identify the parameters of the electrochemical lithium-ion battery model with high calculation accuracy. A new machine learning method was proposed to realize battery health management. An integrated data mining framework was constructed for the battery characteristic expression and prediction [84]. The DL methods perform feature extraction in an effective automated manner using minimal domain knowledge and computation [85].

These methods are realized with a hierarchical data representation architecture to extract the advanced features from the last layer of the network. Additionally, low-level features are extracted from the bottom layer. These types were inspired by AI originally, which has achieved great success in many fields to become one of the most popular research directions in the machine learning society [86]. An overview of DL is obtained from different perspectives, including history, challenges, methods, frameworks, applications, and parallel and distributed computing technologies [87]. Therefore, the DL method was introduced into the RUL prediction process, and its overall framework is presented in Figure 9.

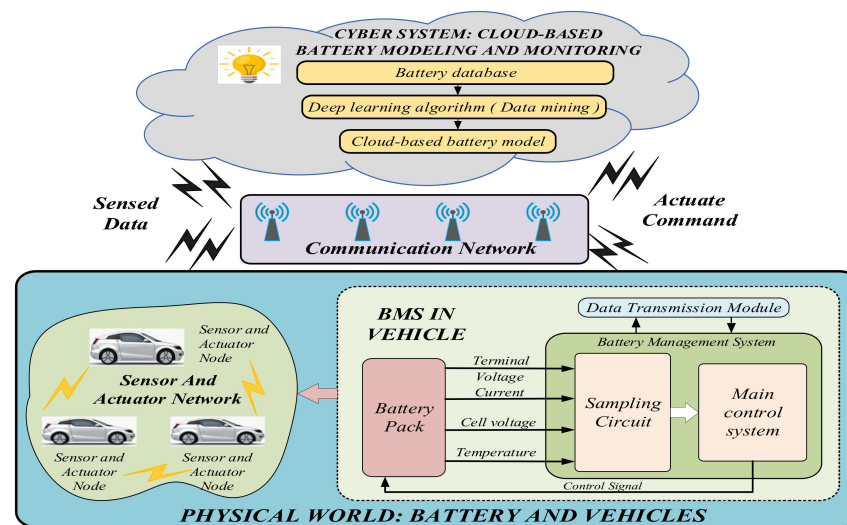


Figure 9. The DL and related method application for the SOH prediction.

In Figure 9, DL-based methods are considered a broad research method, and the biggest challenge is to train them using existing large datasets. As datasets are becoming large, diverse, and complex, the DL method has become a key tool for large-scale data analysis [88]. Challenges and opportunities arise in key areas that should be prioritized, including parallelism, scalability, functionality, and optimization. Different DL networks have been introduced into different application fields, such as RNN, CNN, TensorFlow, and PyTorch methods, to solve this problem [89].

### 3.4. Deep Learning for State Prediction

The DNN and DCNN methods have also been used to predict the SOH of lithium-ion batteries. The 0.5 packet loss technique is also introduced into the network, which is an effective regularization method to avoid the overfitting of training data [90]. The fully connected layer uses the rectifying linear unit (ReLU) activation function to avoid the vanishing of the gradient [91]. The root-mean-square error (RMSE) and normalized root-mean-square error (NRMSE) metrics are used to evaluate the loss function of the network training process. Their mathematical expressions are defined in Equation (15).

$$\begin{cases} \text{RMSE} = \sqrt{\frac{\sum_{i=1}^{N_s} (Y(i) - \hat{Y}(i))^2}{N_s}} \\ \text{NRMSE} = \frac{\sqrt{\frac{1}{N_s} \sum_{i=1}^{N_s} \|Y(i) - \hat{Y}(i)\|_2^2}}{(Y_{\max} - Y_{\min})} \end{cases} \quad (15)$$

where  $N_s$  is the number of data,  $Y(i)$  represents the tag vector for the  $i$ -th sample, and  $\hat{Y}(i)$  denotes the sample prediction result corresponding to this method. In addition to the RMSE and NRMSE, three other metrics are also used to evaluate modeling performance. These metrics are the MAE, maximum absolute error (MaxE), and mean absolute percentage error (MAPE), as shown in Equation (16).

$$\begin{cases} \text{MAE} = \frac{1}{N_s} \sum_{i=1}^{N_s} |Y(i) - \hat{Y}(i)| \\ \text{MaxE} = \text{Max} |Y(i) - \hat{Y}(i)| \\ \text{MAPE} = \frac{1}{N_s} \sum_{i=1}^{N_s} \left| \frac{Y(i) - \hat{Y}(i)}{Y(i)} \right| \end{cases} \quad (16)$$

In Equation (16), the SOH value of the next step of  $np$  is predicted directly from previous measurements made at timepoint  $t$  according to the formula. Therefore, the trained model can easily perform multistep prediction. Furthermore, it is essential to implement the development of long-term SOH prediction online when battery degradation occurs at timepoint  $t$ . The SOH value is accurately predicted and determined in the remaining time before it exceeds the predetermined failure threshold. A moving sliding window scenario for remote health assessment is established, as shown in Figure 10.

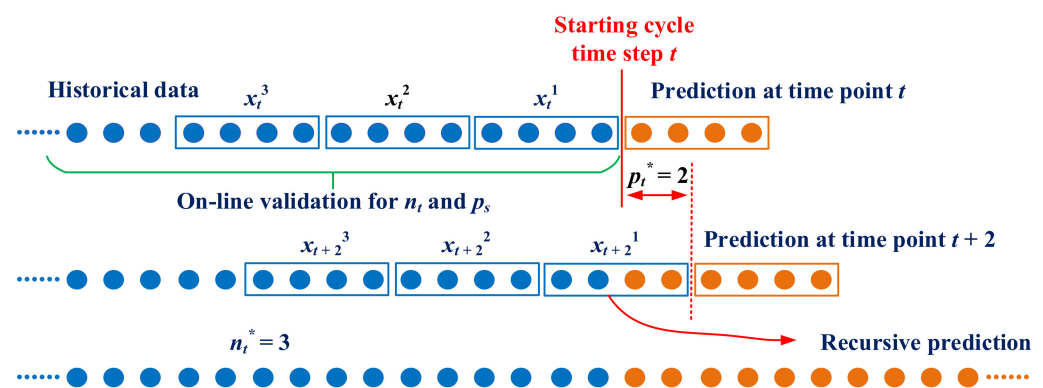


**Figure 10.** Moving sliding window scheme for RUL prediction (“\*” is a special symbol that is used to characterize new values different from  $p$  and  $n$ ).

In Figure 10, the size of the sliding window is  $n_t \times n_s$ , where  $n_t$  is the number of data segments prepared for the estimated sample obtained at timepoint  $t$ . Firstly, a direct multistep advanced SOH prediction is realized at the timepoint  $t$ , and  $Y_t = S(t+k)$  can be obtained at the timepoint  $k = 1, 2, \dots, n_p$ , which indicates the predicted future value from step  $t+1$  to step  $t+np$ . Next, the prediction step is selected on the basis of the prediction scheme. The first  $p_t$  predictor is then merged into the sliding window, and the same number of data points are discarded at the beginning of the sliding window. Multiple steps are repeated in the time window to achieve the long-term SOH prediction [92].

The dual DL coordination control of hybrid ESS is carried out for microgrids. Multi-agent deep reinforcement learning overcomes the demanding response problem for energy management of discrete battery systems [93]. The optimal peak drift of household load is connected to the public power grid by a DL network. An optimized energy storage method based on DL was proposed to realize adaptive dynamic programming [94]. Furthermore, AI and ML methods are applied to the target ESS solution. Reliable power dispatching for emission-free ships is carried out, and constrained charging is realized by the multi-objective deep reinforcement learning (DRL) method [95].

Real-time random ESS optimization is achieved through DPP-based forecasting, residential photovoltaic power generation (RPV), and improved battery energy storage (BES) [96]. A multi-agent reinforcement learning framework was constructed to solve the scheduling problem of lithium-ion batteries [97]. The energy management strategy based on DRL modeling is transferred to hybrid EVs [98]. Deep reinforcement learning

(DRL) and TL are combined with EMS training to perform specific depth deterministic gradient methods at different speed intervals according to the training of the BMS [99]. The energy management of hybrid EVs based on reinforcement learning and dual deep Q learning was carried out, and the dual learning framework is constructed [100]. The LSTM network is used to predict multiple parameters of the EV battery system. The developed pre-loss technology is introduced to prevent the over-fitting phenomenon [101]. The energy management of microgrids is achieved using a DL predictor, in which a multi-agent framework for early scheduling is constructed [102].

On the basis of deep Q-learning and Bayesian optimization, the energy management strategy of EVs is extracted. It is accurate to use the LSTM method to predict battery system faults. The energy management of hybrid EVs is realized by deep reinforcement learning in continuous state-space expression, and the bubble defect detection is implemented by the CNN method [103]. The reinforcement learning of demand response is reviewed. It is considered that reinforcement learning can coordinate multi-agent systems participating in demand response programs [104]. In the absence of observed data, random variables are predicted on the basis of prior distributions. Then, the data is obtained to optimize the prior probability of the random variable [105]. Therefore, the posterior distribution of the random variable  $x$  is obtained by introducing data [106]. These are the equation of state, the observation equation, and the initial value of the probability density.

The mathematical function of the next timepoint is obtained through the observation point prediction. The SOH values observed at time point  $t$  are used to modify and obtain the predicted PDF [107]. The initial equation and a posterior value of the PDF are obtained for the iterative update. On the basis of the initial equation, the probability density formula is converted [108]. The observation factors are independent of each other, leading to the posterior filtering and recursive updating of the PDF [109]. Since the posterior probability density is difficult to obtain, the observation point prediction method needs to be combined with other methods to obtain the PDF.

#### 4. Comparative Analysis of State Prediction Effects Using Different DL Methods

In this section, the key criteria are introduced to compare different models in the literature to find the best method for battery SOH prediction. Then, the research direction of battery state prediction is discussed [110]. The modeling performance and results of different prediction methods are compared. The internal structure is also related to the prediction of the battery state [111]. Parametric models are implemented by changing parameters, which are treated as functional constants. For online learning processes, this limits the adaptability of predictive processes [112]. Therefore, the ability to predict accurately depends on the reliability of the initial model. Because the neural network model also has a fixed weight, it is regarded as a parameterized modeling type [113]. Thus, different DL methods can show different predictive effects. The predicted effects were obtained and compared using RMSE, MaxE, convergence speed, and accuracy as evaluation criteria, as shown in Table 1.

It can be observed from the comparative analysis in Table 1 that the DL method is very effective for the state prediction of lithium-ion batteries. Among them, the DCNN and LSTM methods are mainly used for accurate state prediction. The maximum likelihood method compares the influence of each parameter on the prediction results to evaluate the prediction results. This method's implementation process is effective in random sampling. As a result, a random variable that conforms to the corresponding distribution type must be used. The DCNN-ETL working principle is then applied to achieve an accurate state prediction, thereby validating the experimental test. Lab test data completed throughout the life cycle for over 1 year from 2019 to 2021 are readily available: <https://www.researchgate.net/project/Battery-life-test> and <https://www.researchgate.net/project/Whole-Life-Cycle-Test>. The access date is unlimited.

**Table 1.** The prediction effect comparison results for different DL methods.

Methods	RMSE (%)	MaxE (%)	Convergence Speed (s)	Accuracy (%)
Extreme learning machine (ELM)	-	-	-	94.20
Deep convolutional neural network (DCNN)	1.986	6.838	14.138 s	-
Deep neural network (DNN)	1.59	7.14	-	-
Recurrent neural network (RNN)	6.87	37.92	-	-
DCNN with ensemble transfer learning (DCNN-ETL)	1.114	5.487	133.924	-
DCNN with ensemble learning (DCNN-EL)	3.539	16.798	144.583	-
DCNN with transfer learning (DCNN-TL)	1.361	2.452	12.294	-
Adaptive LSTM (ALSTM)	-	-	46.847	93.12
ALSTM with an attention mechanism	-	-	26.701	97.22
Average Euclidean distance-stacked denoising autoencoder (AED-SDA)	-	-	-	92.40
Gated recurrent unit-Gaussian process regression (GRU-GPR)	0.79	7.92	-	-

## 5. Conclusions

Accurate prediction of battery state is the key to difficult lithium-ion battery state monitoring, and the DL method improves prediction accuracy and robustness. This paper presented a rigorous review, classification, and comparison of DL methods for accurate state prediction. A specific standard was defined to evaluate the accuracy and computational cost of different modeling types. Experimental results showed that the DL method has nonparametric characteristics, probabilistic ability, and strong computational advantages, which makes it suitable for accurate prediction results. The mathematical function constructed is particularly convenient for accurate state prediction and provides an efficient choice of solutions. Recent developments in modeling methods require further research and development. The latest techniques were proposed and compared by providing a simple method to build an adaptive prediction model. Exploratory and adaptive prediction strategies based on DL can promote the popularization and application of the lithium-ion battery. Through the comparison of various improved DL methods, the high-precision DCNN-ELM method was realized and verified in recent studies by reducing the test time, improving the prediction accuracy, and improving the modeling adaptability.

**Author Contributions:** Conceptualization, S.W. and P.R.; methodology, P.T.-A.; software, S.J.; validation, P.T.-A., Carlos Fernandez and S.W.; formal analysis, C.F.; investigation, S.J.; resources, S.J.; data curation, C.F.; writing—original draft preparation, P.R.; writing—review and editing, P.T.-A.; visualization, S.W.; supervision, S.W.; project administration, C.F.; funding acquisition, S.W. All authors have read and agreed to the published version of the manuscript.

**Funding:** This research was funded by [National Natural Science Foundation of China] grant number [62173281].

**Institutional Review Board Statement:** Not applicable.

**Informed Consent Statement:** Not applicable.

**Data Availability Statement:** The data presented in this study are openly available on Reaserchgate: <https://www.researchgate.net/project/Battery-life-test> and <https://www.researchgate.net/project/Whole-Life-Cycle-Test>.

**Acknowledgments:** This work was supported by the National Natural Science Foundation of China (No. 62173281, 61801407), the Sichuan Science and Technology Program (No. 2019YFG0427), the China Scholarship Council (No. 201908515099), and the Fund of Robot Technology used for the Special Environment Key Laboratory of Sichuan Province (No. 18kftk03). Carlos Fernandez also expresses his profound gratitude to Robert Gordon University and, in particular, to PALS for the support.

**Conflicts of Interest:** The authors declare no conflict of interest.

## References

1. Xiong, R.; Li, L.; Tian, J. Towards a smarter battery management system: A critical review on battery state of health monitoring methods. *J. Power Sources* **2018**, *405*, 18–29. [\[CrossRef\]](#)
2. Ren, H.B.; Zhao, Y.Z.; Chen, S.Z.; Wang, T.P. Design and implementation of a battery management system with active charge balance based on the SOC and SOH online estimation. *Energy* **2019**, *166*, 908–917. [\[CrossRef\]](#)
3. Cen, Z.H.; Kubiak, P. Lithium-ion battery SOC/SOH adaptive estimation via simplified single particle model. *Int. J. Energy Res.* **2020**, *44*, 12444–12459. [\[CrossRef\]](#)
4. Li, S.; Li, K.; Xiao, E.; Wong, C.-K. Joint SoC and SoH Estimation for Zinc–Nickel Single-Flow Batteries. *IEEE Trans. Ind. Electron.* **2020**, *67*, 8484–8494. [\[CrossRef\]](#)
5. Feng, Y.; Xue, C.; Han, Q.; Han, F.; Du, J. Robust Estimation for State-of-Charge and State-of-Health of Lithium-Ion Batteries Using Integral-Type Terminal Sliding-Mode Observers. *IEEE Trans. Ind. Electron.* **2020**, *67*, 4013–4023. [\[CrossRef\]](#)
6. Hu, X.; Yuan, H.; Zou, C.; Li, Z.; Zhang, L. Co-Estimation of State of Charge and State of Health for Lithium-Ion Batteries Based on Fractional-Order Calculus. *IEEE Trans. Veh. Technol.* **2018**, *67*, 10319–10329. [\[CrossRef\]](#)
7. Shen, P.; Ouyang, M.; Lu, L.; Li, J.; Feng, X. The Co-estimation of State of Charge, State of Health, and State of Function for Lithium-Ion Batteries in Electric Vehicles. *IEEE Trans. Veh. Technol.* **2018**, *67*, 92–103. [\[CrossRef\]](#)
8. Hu, X.; Feng, F.; Liu, K.; Zhang, L.; Xie, J.; Liu, B. State estimation for advanced battery management: Key challenges and future trends. *Renew. Sustain. Energy Rev.* **2019**, *114*, 109334. [\[CrossRef\]](#)
9. Kawahara, Y.; Sakabe, K.; Nakao, R.; Tsuru, K.; Okawa, K.; Aoshima, Y.; Kudo, A.; Emori, A. Development of status detection method of lithium-ion rechargeable battery for hybrid electric vehicles. *J. Power Sources* **2021**, *481*, 228760. [\[CrossRef\]](#)
10. Wang, S.; Takyi-Aninakwa, P.; Fan, Y.; Yu, C.; Jin, S.; Fernandez, C.; Stroe, D.-I. A novel feedback correction-adaptive Kalman filtering method for the whole-life-cycle state of charge and closed-circuit voltage prediction of lithium-ion batteries based on the second-order electrical equivalent circuit model. *Int. J. Electr. Power.* **2022**, *139*, 108020. [\[CrossRef\]](#)
11. Xiao, D.; Fang, G.; Liu, S.; Yuan, S.; Ahmed, R.; Habibi, S.; Emadi, A. Reduced-Coupling Coestimation of SOC and SOH for Lithium-Ion Batteries Based on Convex Optimization. *IEEE Trans. Power Electron.* **2020**, *35*, 12332–12346. [\[CrossRef\]](#)
12. Zhang, Q.; Wang, D.; Yang, B.; Cui, X.; Li, X. Electrochemical model of lithium-ion battery for wide frequency range applications. *Electrochim. Acta* **2020**, *343*, 136094. [\[CrossRef\]](#)
13. Yang, F.; Li, W.; Li, C.; Miao, Q. State-of-charge estimation of lithium-ion batteries based on gated recurrent neural network. *Energy* **2019**, *175*, 66–75. [\[CrossRef\]](#)
14. Wang, S.-L.; Fernandez, C.; Zou, C.-Y.; Yu, C.-M.; Chen, L.; Zhang, L. A comprehensive working state monitoring method for power battery packs considering state of balance and aging correction. *Energy* **2019**, *171*, 444–455. [\[CrossRef\]](#)
15. Wang, Y.; Gao, G.; Li, X.; Chen, Z. A fractional-order model-based state estimation approach for lithium-ion battery and ultra-capacitor hybrid power source system considering load trajectory. *J. Power Sources* **2020**, *449*, 227543. [\[CrossRef\]](#)
16. Song, Y.; Liu, D.; Liao, H.; Peng, Y. A hybrid statistical data-driven method for on-line joint state estimation of lithium-ion batteries. *Appl. Energy* **2020**, *261*, 114408. [\[CrossRef\]](#)
17. Linghu, J.; Kang, L.; Liu, M.; Luo, X.; Feng, Y.; Lu, C. Estimation for state-of-charge of lithium-ion battery based on an adaptive high-degree cubature Kalman filter. *Energy* **2019**, *189*, 116204. [\[CrossRef\]](#)
18. Liu, G.; Xu, C.; Li, H.; Jiang, K.; Wang, K. State of charge and online model parameters co-estimation for liquid metal batteries. *Appl. Energy* **2019**, *250*, 677–684. [\[CrossRef\]](#)
19. Chen, Z.; Sun, H.; Dong, G.; Wei, J.; Wu, J. Particle filter-based state-of-charge estimation and remaining-dischargeable-time prediction method for lithium-ion batteries. *J. Power Sources* **2019**, *414*, 158–166. [\[CrossRef\]](#)
20. Feng, F.; Teng, S.; Liu, K.; Xie, J.; Xie, Y.; Liu, B.; Li, K. Co-estimation of lithium-ion battery state of charge and state of temperature based on a hybrid electrochemical-thermal-neural-network model. *J. Power Sources* **2020**, *455*, 227935. [\[CrossRef\]](#)
21. Li, W.; Rentemeister, M.; Badeda, J.; Jost, D.; Schulte, D.; Sauer, D.U. Digital twin for battery systems: Cloud battery management system with online state-of-charge and state-of-health estimation. *J. Energy Storage* **2020**, *30*, 101557. [\[CrossRef\]](#)
22. Wang, Y.; Chen, Z. A framework for state-of-charge and remaining discharge time prediction using unscented particle filter. *Appl. Energy* **2020**, *260*, 114324. [\[CrossRef\]](#)
23. Wei, Z.; Dong, G.; Zhang, X.; Pou, J.; Quan, Z.; He, H. Noise-Immune Model Identification and State-of-Charge Estimation for Lithium-Ion Battery Using Bilinear Parameterization. *IEEE Trans. Ind. Electron.* **2021**, *68*, 312–323. [\[CrossRef\]](#)
24. Chen, Z.G.; Zhou, J.X.; Zhou, F.; Xu, S. State-of-charge estimation of lithium-ion batteries based on improved H infinity filter algorithm and its novel equalization method. *J. Clean. Prod.* **2021**, *290*, 15. [\[CrossRef\]](#)
25. Ma, C.; Zhai, X.; Wang, Z.; Tian, M.; Yu, Q.; Liu, L.; Liu, H.; Wang, H.; Yang, X. State of health prediction for lithium-ion batteries using multiple-view feature fusion and support vector regression ensemble. *Int. J. Mach. Learn. Cybern.* **2019**, *10*, 2269–2282. [\[CrossRef\]](#)
26. Ungurean, L.; Micea, M.V.; Cârstoiu, G. Online state of health prediction method for lithium-ion batteries, based on gated recurrent unit neural networks. *Int. J. Energy Res.* **2020**, *44*, 6767–6777. [\[CrossRef\]](#)
27. Li, P.; Zhang, Z.; Xiong, Q.; Ding, B.; Hou, J.; Luo, D.; Rong, Y.; Li, S. State-of-health estimation and remaining useful life prediction for the lithium-ion battery based on a variant long short term memory neural network. *J. Power Sources* **2020**, *459*, 228069. [\[CrossRef\]](#)

28. He, L.; Yang, Z.; Gu, Y.; Liu, C.; He, T.; Shin, K.G. SoH-Aware Reconfiguration in Battery Packs. *IEEE Trans. Smart Grid* **2018**, *9*, 3727–3735. [[CrossRef](#)]
29. He, J.; Wei, Z.; Bian, X.; Yan, F. State-of-Health Estimation of Lithium-Ion Batteries Using Incremental Capacity Analysis Based on Voltage–Capacity Model. *IEEE Trans. Transp. Electrification* **2020**, *6*, 417–426. [[CrossRef](#)]
30. Lajara, R.; Pérez-Solano, J.J.; Pelegrí-Sebastiá, J. Predicting the Batteries’ State of Health in Wireless Sensor Networks Applications. *IEEE Trans. Ind. Electron.* **2018**, *65*, 8936–8945. [[CrossRef](#)]
31. Tian, J.; Xiong, R.; Shen, W. State-of-Health Estimation Based on Differential Temperature for Lithium Ion Batteries. *IEEE Trans. Power Electron.* **2020**, *35*, 10363–10373. [[CrossRef](#)]
32. Dong, G.; Chen, Z.; Wei, J.; Ling, Q. Battery Health Prognosis Using Brownian Motion Modeling and Particle Filtering. *IEEE Trans. Ind. Electron.* **2018**, *65*, 8646–8655. [[CrossRef](#)]
33. Stroe, D.; Schaltz, E. Lithium-Ion Battery State-of-Health Estimation Using the Incremental Capacity Analysis Technique. *IEEE Trans. Ind. Appl.* **2020**, *56*, 678–685. [[CrossRef](#)]
34. Guha, A.; Patra, A. State of Health Estimation of Lithium-Ion Batteries Using Capacity Fade and Internal Resistance Growth Models. *IEEE Trans. Transp. Electrification* **2018**, *4*, 135–146. [[CrossRef](#)]
35. Leijen, P.; Steyn-Ross, D.A.; Kularatna, N. Use of Effective Capacitance Variation as a Measure of State-of-Health in a Series-Connected Automotive Battery Pack. *IEEE Trans. Veh. Technol.* **2018**, *67*, 1961–1968. [[CrossRef](#)]
36. Hametner, C.; Jakubek, S.; Prochazka, W. Data-Driven Design of a Cascaded Observer for Battery State of Health Estimation. *IEEE Trans. Ind. Appl.* **2018**, *54*, 6258–6266. [[CrossRef](#)]
37. Ma, Z.; Gao, F.; Gu, X.; Li, N.; Wu, Q.; Wang, X.; Wang, X. Multilayer SOH Equalization Scheme for MMC Battery Energy Storage System. *IEEE Trans. Power Electron.* **2020**, *35*, 13514–13527. [[CrossRef](#)]
38. Dai, H.D.; Zhao, G.C.; Lin, M.Q.; Wu, J.; Zheng, G.F. A Novel Estimation Method for the State of Health of Lithium-Ion Battery Using Prior Knowledge-Based Neural Network and Markov Chain. *IEEE Trans. Ind. Electron.* **2019**, *66*, 7706–7716. [[CrossRef](#)]
39. Mawonou, K.S.R.; Eddahech, A.; Dumur, D.; Beauvois, D.; Godoy, E. State-of-health estimators coupled to a random forest approach for lithium-ion battery aging factor ranking. *J. Power Sources* **2021**, *484*, 229154. [[CrossRef](#)]
40. Zhou, D.; Zheng, W.; Chen, S.; Fu, P.; Zhu, H.; Song, B.; Qu, X.; Wang, T. Research on state of health prediction model for lithium batteries based on actual diverse data. *Energy* **2021**, *230*, 120851. [[CrossRef](#)]
41. Chen, W.; Xu, C.; Chen, M.; Jiang, K.; Wang, K. A novel fusion model based online state of power estimation method for lithium-ion capacitor. *J. Energy Storage* **2021**, *36*, 102387. [[CrossRef](#)]
42. Esfandyari, M.J.; Esfahanian, V.; Yazdi, M.R.H.; Nehzati, H.; Shekoofa, O. A new approach to consider the influence of aging state on Lithium-ion battery state of power estimation for hybrid electric vehicle. *Energy* **2019**, *176*, 505–520. [[CrossRef](#)]
43. Esfandyari, M.J.; Yazdi, M.R.H.; Esfahanian, V.; Masih-Tehrani, M.; Nehzati, H.; Shekoofa, O. A hybrid model predictive and fuzzy logic based control method for state of power estimation of series-connected Lithium-ion batteries in HEVs. *J. Energy Storage* **2019**, *24*, 100758. [[CrossRef](#)]
44. Tang, X.; Wang, Y.; Yao, K.; He, Z.; Gao, F. Model migration based battery power capability evaluation considering uncertainties of temperature and aging. *J. Power Sources* **2019**, *440*, 227141. [[CrossRef](#)]
45. Takyi-Aninakwa, P.; Wang, S.; Zhang, H.; Appiah, E.; Boboee, E.D.; Fernandez, C. A strong tracking adaptive fading-extended Kalman filter for the state of charge estimation of lithium-ion batteries. *Int. J. Energy Res.* **2022**, *47*, 1–18. [[CrossRef](#)]
46. Hu, X.; Jiang, H.; Feng, F.; Liu, B. An enhanced multi-state estimation hierarchy for advanced lithium-ion battery management. *Appl. Energy* **2020**, *257*, 114019. [[CrossRef](#)]
47. Verma, M.K.S.; Basu, S.; Patil, R.S.; Hariharan, K.S.; Adiga, S.P.; Kolake, S.M.; Oh, D.; Song, T.; Sung, Y. On-Board State Estimation in Electrical Vehicles: Achieving Accuracy and Computational Efficiency Through an Electrochemical Model. *IEEE Trans. Veh. Technol.* **2020**, *69*, 2563–2575. [[CrossRef](#)]
48. Lai, X.; He, L.; Wang, S.; Zhou, L.; Zhang, Y.; Sun, T.; Zheng, Y. Co-estimation of state of charge and state of power for lithium-ion batteries based on fractional variable-order model. *J. Clean. Prod.* **2020**, *255*, 120203. [[CrossRef](#)]
49. Wang, Y.; Tian, J.; Sun, Z.; Wang, L.; Xu, R.; Li, M.; Chen, Z. A comprehensive review of battery modeling and state estimation approaches for advanced battery management systems. *Renew. Sustain. Energy Rev.* **2020**, *131*, 110015. [[CrossRef](#)]
50. Lin, P.; Jin, P.; Hong, J.; Wang, Z. Battery voltage and state of power prediction based on an improved novel polarization voltage model. *Energy Rep.* **2020**, *6*, 2299–2308. [[CrossRef](#)]
51. Shrivastava, P.; Soon, T.K.; Bin Idris, M.Y.I.; Mekhilef, S.; Adnan, S.B.R.S. Model-based state of X estimation of lithium-ion battery for electric vehicle applications. *Int. J. Energy Res.* **2022**, *46*, 10704–10723. [[CrossRef](#)]
52. Zhou, W.; Zhang, N.; Zhai, H. Enhanced Battery Power Constraint Handling in MPC-Based HEV Energy Management: A Two-Phase Dual-Model Approach. *IEEE Trans. Transp. Electrification* **2021**, *7*, 1236–1248. [[CrossRef](#)]
53. Tang, X.; Liu, K.; Liu, Q.; Peng, Q.; Gao, F. Comprehensive study and improvement of experimental methods for obtaining referenced battery state-of-power. *J. Power Sources* **2021**, *512*, 230462. [[CrossRef](#)]
54. An, F.; Jiang, J.; Zhang, W.; Zhang, C.; Fan, X. State of Energy Estimation for Lithium-Ion Battery Pack via Prediction in Electric Vehicle Applications. *IEEE Trans. Veh. Technol.* **2022**, *71*, 184–195. [[CrossRef](#)]
55. Chen, Y.; Yang, X.; Luo, D.; Wen, R. Remaining available energy prediction for lithium-ion batteries considering electrothermal effect and energy conversion efficiency. *J. Energy Storage* **2021**, *40*, 102728. [[CrossRef](#)]

56. Ezemobi, E.; Silvagni, M.; Mozaffari, A.; Tonoli, A.; Khajepour, A. State of Health Estimation of Lithium-Ion Batteries in Electric Vehicles under Dynamic Load Conditions. *Energies* **2022**, *15*, 1234. [[CrossRef](#)]
57. Lai, X.; Huang, Y.; Han, X.; Gu, H.; Zheng, Y. A novel method for state of energy estimation of lithium-ion batteries using particle filter and extended Kalman filter. *J. Energy Storage* **2021**, *43*, 103269. [[CrossRef](#)]
58. Shrivastava, P.; Kok Soon, T.; Bin Idris, M.Y.I.; Mekhilef, S.; Adnan, S.B.R.S. Combined State of Charge and State of Energy Estimation of Lithium-Ion Battery Using Dual Forgetting Factor-Based Adaptive Extended Kalman Filter for Electric Vehicle Applications. *IEEE Trans. Veh. Technol.* **2021**, *70*, 1200–1215. [[CrossRef](#)]
59. Tang, D.Y.; Gong, M.T.; Yu, J.S.; Li, X. A power transfer model-based method for lithium-ion battery discharge time prediction of electric rotatory-wing UAV. *Microelectron. Reliab.* **2020**, *114*, 113832. [[CrossRef](#)]
60. Wei, X.; Jun, C.; Yu, G.; Ma, J.M.; Chang, J. Unscented Particle Filter Based State of Energy Estimation for LiFePO<sub>4</sub> Batteries Using an Online Updated Model. *Int. J. Automot. Technol.* **2022**, *23*, 503–510. [[CrossRef](#)]
61. Zhang, S.; Peng, N.; Zhang, X. An application-oriented multistate estimation framework of lithium-ion battery used in electric vehicles. *Int. J. Energy Res.* **2021**, *45*, 18554–18576. [[CrossRef](#)]
62. Zhang, S.; Zhang, X. Joint estimation method for maximum available energy and state-of-energy of lithium-ion battery under various temperatures. *J. Power Sources* **2021**, *506*, 230132. [[CrossRef](#)]
63. Zhang, S.; Zhang, X. A novel low-complexity state-of-energy estimation method for series-connected lithium-ion battery pack based on “representative cell” selection and operating mode division. *J. Power Sources* **2022**, *518*, 230732. [[CrossRef](#)]
64. Zhang, S.; Zhang, X. A novel non-experiment-based reconstruction method for the relationship between open-circuit-voltage and state-of-charge/state-of-energy of lithium-ion battery. *Electrochim. Acta* **2022**, *403*, 139637. [[CrossRef](#)]
65. Huang, Y.; Tang, Y.; VanZwieten, J. Prognostics With Variational Autoencoder by Generative Adversarial Learning. *IEEE Trans. Ind. Electron.* **2022**, *69*, 856–867. [[CrossRef](#)]
66. Khaleghi, S.; Hosen, M.S.; Karimi, D.; Behi, H.; Beheshti, S.H.; Van Mierlo, J.; Bercebar, M. Developing an online data-driven approach for prognostics and health management of lithium-ion batteries. *Appl. Energy* **2022**, *308*, 118348. [[CrossRef](#)]
67. Lin, C.P.; Ling, M.H.; Cabrera, J.; Yang, F.; Yu, D.Y.W.; Tsui, K.L. Prognostics for lithium-ion batteries using a two-phase gamma degradation process model. *Reliab. Eng. Syst. Saf.* **2021**, *214*, 107797. [[CrossRef](#)]
68. Nagulapati, V.M.; Lee, H.; Jung, D.; Brigljevic, B.; Choi, Y.; Lim, H. Capacity estimation of batteries: Influence of training dataset size and diversity on data driven prognostic models. *Reliab. Eng. Syst. Saf.* **2021**, *216*, 108048. [[CrossRef](#)]
69. Weddington, J.; Niu, G.; Chen, R.; Yan, W.; Zhang, B. Lithium-ion battery diagnostics and prognostics enhanced with Dempster-Shafer decision fusion. *Neurocomputing* **2021**, *458*, 440–453. [[CrossRef](#)]
70. Yang, Y. A machine-learning prediction method of lithium-ion battery life based on charge process for different applications. *Appl. Energy* **2021**, *292*, 116897. [[CrossRef](#)]
71. Camargos, M.O.; Bessa, I.; Silveira Vasconcelos D’Angelo, M.F.; Cosme, L.B.; Palhares, R.M. Data-driven prognostics of rolling element bearings using a novel Error Based Evolving Takagi-Sugeno Fuzzy Model. *Appl. Soft Comput.* **2020**, *96*, 106628. [[CrossRef](#)]
72. Dong, G.; Yang, F.; Wei, Z.; Wei, J.; Tsui, K.-L. Data-Driven Battery Health Prognosis Using Adaptive Brownian Motion Model. *IEEE Trans. Ind. Inform.* **2020**, *16*, 4736–4746. [[CrossRef](#)]
73. Li, X.; Huang, Z.; Tian, J.; Tian, Y. State-of-charge estimation tolerant of battery aging based on a physics-based model and an adaptive cubature Kalman filter. *Energy* **2021**, *220*, 119767. [[CrossRef](#)]
74. Lin, C.P.; Cabrera, J.; Yang, F.F.; Ling, M.H.; Tsui, K.L.; Bae, S.J. Battery state of health modeling and remaining useful life prediction through time series model. *Appl. Energy* **2020**, *275*, 115338. [[CrossRef](#)]
75. Zhang, Y.Z.; Xiong, R.; He, H.W.; Qu, X.B.; Pecht, M. State of charge-dependent aging mechanisms in graphite/Li(NiCoAl)O<sub>2</sub> cells: Capacity loss modeling and remaining useful life prediction. *Appl. Energy* **2019**, *255*, 113818. [[CrossRef](#)]
76. Zhao, Y.; Stein, P.; Bai, Y.; Al-Siraj, M.; Yang, Y.Y.W.; Xu, B.X. A review on modeling of electro-chemo-mechanics in lithium-ion batteries. *J. Power Sources* **2019**, *413*, 259–283. [[CrossRef](#)]
77. Zhu, J.G.; Knapp, M.; Darma, M.S.D.; Fang, Q.H.; Wang, X.Y.; Dai, H.F.; Wei, X.Z.; Ehrenberg, H. An improved electro-thermal battery model complemented by current dependent parameters for vehicular low temperature application. *Appl. Energy* **2019**, *248*, 149–161. [[CrossRef](#)]
78. Farmann, A.; Sauer, D.U. Comparative study of reduced order equivalent circuit models for on-board state-of-available-power prediction of lithium-ion batteries in electric vehicles. *Appl. Energy* **2018**, *225*, 1102–1122. [[CrossRef](#)]
79. Yang, X.; Wang, S.; Xu, W.; Qiao, J.; Yu, C.; Takyi-Aninakwa, P.; Jin, S. A novel fuzzy adaptive cubature Kalman filtering method for the state of charge and state of energy co-estimation of lithium-ion batteries. *Electrochim. Acta* **2022**, *415*, 140241. [[CrossRef](#)]
80. Liu, K.L.; Ashwin, T.R.; Hu, X.S.; Lucu, M.; Widanage, W.D. An evaluation study of different modelling techniques for calendar ageing prediction of lithium-ion batteries. *Renew. Sustain. Energy Rev.* **2020**, *131*, 110017. [[CrossRef](#)]
81. Qiao, J.; Wang, S.; Yu, C.; Yang, X.; Fernandez, C. A novel intelligent weight decreasing firefly-particle filtering method for accurate state-of-charge estimation of lithium-ion batteries. *Int. J. Energy Res.* **2022**, *46*, 6613–6622. [[CrossRef](#)]

82. Zhang, Y.Z.; Xiong, R.; He, H.W.; Pecht, M.G. Long Short-Term Memory Recurrent Neural Network for Remaining Useful Life Prediction of Lithium-Ion Batteries. *IEEE Trans. Veh. Technol.* **2018**, *67*, 5695–5705. [[CrossRef](#)]
83. Zhao, R.X.; Kollmeyer, P.J.; Lorenz, R.D.; Jahns, T.M. A Compact Methodology Via a Recurrent Neural Network for Accurate Equivalent Circuit Type Modeling of Lithium-Ion Batteries. *IEEE Trans. Ind. Appl.* **2019**, *55*, 1922–1931. [[CrossRef](#)]
84. Chehade, A.A.; Hussein, A.A. A Collaborative Gaussian Process Regression Model for Transfer Learning of Capacity Trends Between Li-Ion Battery Cells. *IEEE Trans. Veh. Technol.* **2020**, *69*, 9542–9552. [[CrossRef](#)]
85. Du, J.; Liu, Y.; Mo, X.; Li, Y.; Li, J.; Wu, X.; Ouyang, M. Impact of high-power charging on the durability and safety of lithium batteries used in long-range battery electric vehicles. *Appl. Energy* **2019**, *255*, 113793. [[CrossRef](#)]
86. Eleftheroglou, N.; Mansouri, S.S.; Loutas, T.; Karvelis, P.; Georgoulas, G.; Nikolakopoulos, G.; Zarouchas, D. Intelligent data-driven prognostic methodologies for the real-time remaining useful life until the end-of-discharge estimation of the Lithium-Polymer batteries of unmanned aerial vehicles with uncertainty quantification. *Appl. Energy* **2019**, *254*, 113677. [[CrossRef](#)]
87. Li, X.Y.; Yuan, C.G.; Wang, Z.P. Multi-time-scale framework for prognostic health condition of lithium battery using modified Gaussian process regression and nonlinear regression. *J. Power Sources* **2020**, *467*, 228358. [[CrossRef](#)]
88. Liu, K.L.; Hu, X.S.; Wei, Z.B.; Li, Y.; Jiang, Y. Modified Gaussian Process Regression Models for Cyclic Capacity Prediction of Lithium-Ion Batteries. *IEEE Trans. Transp. Electr.* **2019**, *5*, 1225–1236. [[CrossRef](#)]
89. Lipu, M.S.H.; Hannan, M.A.; Hussain, A.; Hoque, M.M.; Ker, P.J.; Saad, M.H.M.; Ayob, A. A review of state of health and remaining useful life estimation methods for lithium-ion battery in electric vehicles: Challenges and recommendations. *J. Clean. Prod.* **2018**, *205*, 115–133. [[CrossRef](#)]
90. Xiong, R.; Pan, Y.; Shen, W.; Li, H.; Sun, F. Lithium-ion battery aging mechanisms and diagnosis method for automotive applications: Recent advances and perspectives. *Renew. Sustain. Energy Rev.* **2020**, *131*, 110048. [[CrossRef](#)]
91. Yin, L.F.; Gao, Q.; Zhao, L.L.; Wang, T. Expandable deep learning for real-time economic generation dispatch and control of three-state energies based future smart grids. *Energy* **2020**, *191*, 116561. [[CrossRef](#)]
92. Zhang, S.; Guo, X.; Zhang, X. Multi-objective decision analysis for data-driven based estimation of battery states: A case study of remaining useful life estimation. *Int. J. Hydrogen Energy* **2020**, *45*, 14156–14173. [[CrossRef](#)]
93. Hafiz, F.; Awal, M.A.; de Queiroz, A.R.; Husain, I. Real-Time Stochastic Optimization of Energy Storage Management Using Deep Learning-Based Forecasts for Residential PV Applications. *IEEE Trans. Ind. Appl.* **2020**, *56*, 2216–2226. [[CrossRef](#)]
94. Lan, T.; Jermsittiparsert, K.; Alrashood, S.T.; Rezaei, M.; Al-Ghussain, L.; Mohamed, M.A. An advanced machine learning based energy management of renewable microgrids considering hybrid electric vehicles' charging demand. *Energies* **2021**, *14*, 569. [[CrossRef](#)]
95. Lee, C.; Jo, S.; Kwon, D.; Pecht, M.G. Capacity-Fading Behavior Analysis for Early Detection of Unhealthy Li-Ion Batteries. *IEEE Trans. Ind. Electron.* **2021**, *68*, 2659–2666. [[CrossRef](#)]
96. Lin, K.; Chen, Y.; Liu, Y.; Zhang, B. Reliability Prediction of Battery Management System for Electric Vehicles Based on Accelerated Degradation Test: A Semi-Parametric Approach. *IEEE Trans. Veh. Technol.* **2020**, *69*, 12694–12704. [[CrossRef](#)]
97. Liu, J.; Jia, R.; Li, W.; Ma, F.; Abdullah, H.M.; Ma, H.; Mohamed, M.A. High precision detection algorithm based on improved RetinaNet for defect recognition of transmission lines. *Energy Rep.* **2020**, *6*, 2430–2440. [[CrossRef](#)]
98. Meng, F.; Zou, Q.; Zhang, Z.; Wang, B.; Ma, H.; Abdullah, H.M.; Almalaq, A.; Mohamed, M.A. An intelligent hybrid wavelet-adversarial deep model for accurate prediction of solar power generation. *Energy Rep.* **2021**, *7*, 2155–2164. [[CrossRef](#)]
99. Ng, M.F.; Zhao, J.; Yan, Q.Y.; Conduit, G.J.; Seh, Z.W. Predicting the state of charge and health of batteries using data-driven machine learning. *Nat. Mach. Intell.* **2020**, *2*, 161–170. [[CrossRef](#)]
100. Shen, S.; Sadoughi, M.; Li, M.; Wang, Z.D.; Hu, C. Deep convolutional neural networks with ensemble learning and transfer learning for capacity estimation of lithium-ion batteries. *Appl. Energy* **2020**, *260*, 114296. [[CrossRef](#)]
101. Shin, M.; Kim, J.; Levorato, M. Auction-Based Charging Scheduling With Deep Learning Framework for Multi-Drone Networks. *IEEE Trans. Veh. Technol.* **2019**, *68*, 4235–4248. [[CrossRef](#)]
102. Tagade, P.; Hariharan, K.S.; Ramachandran, S.; Khandelwal, A.; Naha, A.; Kolake, S.M.; Han, S.H. Deep Gaussian process regression for lithium-ion battery health prognosis and degradation mode diagnosis. *J. Power Sources* **2020**, *445*, 227281. [[CrossRef](#)]
103. Tian, H.X.; Qin, P.L.; Li, K.; Zhao, Z. A review of the state of health for lithium-ion batteries: Research status and suggestions. *J. Clean. Prod.* **2020**, *261*, 120813. [[CrossRef](#)]
104. Wu, C.; Zhang, L.; Li, Q.S.; Fu, Z.Y.; Zhu, W.W.; Zhang, Y.X. Enabling Flexible Resource Allocation in Mobile Deep Learning Systems. *IEEE Trans. Parallel Distrib. Syst.* **2019**, *30*, 346–360. [[CrossRef](#)]
105. Xu, T.; Peng, Z.; Wu, L. A novel data-driven method for predicting the circulating capacity of lithium-ion battery under random variable current. *Energy* **2021**, *218*, 119530. [[CrossRef](#)]
106. Zhang, Y.W.; Tang, Q.C.; Zhang, Y.; Wang, J.B.; Stimming, U.; Lee, A.A. Identifying degradation patterns of lithium ion batteries from impedance spectroscopy using machine learning. *Nat. Commun.* **2020**, *11*, 1706. [[CrossRef](#)]
107. Zou, H.; Tao, J.; Elsayed, S.K.; Elattar, E.E.; Almalaq, A.; Mohamed, M.A. Stochastic multi-carrier energy management in the smart islands using reinforcement learning and unscented transform. *Int. J. Electr. Power Energy Syst.* **2021**, *130*, 106988. [[CrossRef](#)]
108. Anseán, D.; García, V.M.; González, M.; Blanco-Viejo, C.; Viera, J.C.; Pulido, Y.F.; Sánchez, L. Lithium-Ion Battery Degradation Indicators Via Incremental Capacity Analysis. *IEEE Trans. Ind. Appl.* **2019**, *55*, 2992–3002. [[CrossRef](#)]
109. Chen, L.; Wang, H.M.; Liu, B.H.; Wang, Y.J.; Ding, Y.H.; Pan, H.H. Battery state-of-health estimation based on a metabolic extreme learning machine combining degradation state model and error compensation. *Energy* **2021**, *215*, 119078. [[CrossRef](#)]

110. Corno, M.; Pozzato, G. Active Adaptive Battery Aging Management for Electric Vehicles. *IEEE Trans. Veh. Technol.* **2020**, *69*, 258–269. [[CrossRef](#)]
111. Finegan, D.P.; Zhu, J.; Feng, X.; Keyser, M.; Ulmefors, M.; Li, W.; Bazant, M.Z.; Cooper, S.J. The Application of Data-Driven Methods and Physics-Based Learning for Improving Battery Safety. *Joule* **2020**, *5*, 316–329. [[CrossRef](#)]
112. Li, W.H.; Sengupta, N.; Dechent, P.; Howey, D.; Annaswamy, A.; Sauer, D.U. Online capacity estimation of lithium-ion batteries with deep long short-term memory networks. *J. Power Sources* **2021**, *482*, 228863. [[CrossRef](#)]
113. Li, Y.; Li, K.; Liu, X.; Wang, Y.; Zhang, L. Lithium-ion battery capacity estimation—A pruned convolutional neural network approach assisted with transfer learning. *Appl. Energy* **2021**, *285*, 116410. [[CrossRef](#)]